

# 1 Are seamounts refuge areas for fauna from polymetallic 2 nodule fields?

3 Daphne Cuvelier<sup>1\*</sup>, Pedro A. Ribeiro<sup>1,2\*</sup>, Sofia P. Ramalho<sup>1,3\*</sup>, Daniel Kersken<sup>4,5</sup>, Pedro Martinez  
4 Arbizu<sup>5</sup>, Ana Colaço<sup>1</sup>

5 <sup>1</sup> MARE – Marine and environmental sciences centre/IMAR – Instituto do Mar/Centro OKEANOS –  
6 Universidade dos Açores, Rua Prof. Dr. Frederico Machado 4, 9901-862 Horta, Portugal

7 <sup>2</sup> Current address: Department of Biological Sciences and K.G. Jebsen Centre for Deep-Sea Research,  
8 University of Bergen, Bergen, Norway.

9 <sup>3</sup> Current address: Departamento de Biologia & CESAM, Universidade de Aveiro, Campus  
10 Universitário de Santiago, 3810-193 Aveiro, Portugal

11 <sup>4</sup> Department of Marine Zoology, Senckenberg Research Institute and Natural History Museum,  
12 Senckenberganlage 25, 60325 Frankfurt am Main, Germany

13 <sup>5</sup> German Centre for Marine Biodiversity Research (DZMB), Senckenberg am Meer, Südstrand 44,  
14 26382 Wilhelmshaven, Germany

15 \* Contributed equally to this work/Corresponding authors: Daphne Cuvelier  
16 ([daphne.cuvelier@gmail.com](mailto:daphne.cuvelier@gmail.com)), Pedro Ribeiro ([Pedro.Ribeiro@uib.no](mailto:Pedro.Ribeiro@uib.no)) and Sofia Pinto Ramalho  
17 ([sofia.pinto.ramalho@gmail.com](mailto:sofia.pinto.ramalho@gmail.com))

18 Running title: Seamounts as refuge areas for nodule fauna

19 Six keywords: megafauna, seamounts, nodule fields, image analysis, deep sea, mining

## 20 Abstract

21 Seamounts are abundant and prominent features on the deep-sea floor and intersperse with the  
22 nodule fields of the Clarion-Clipperton Fracture Zone (CCZ). There is a particular interest in  
23 characterising the fauna inhabiting seamounts in the CCZ because they are the only other ecosystem  
24 in the region to provide hard substrata besides the abundant nodules on the soft sediment abyssal  
25 plains. It has been hypothesised that seamounts could provide refuge for organisms during deep-sea  
26 mining actions or that they could play a role in the (re-)colonisation of the disturbed nodule fields.  
27 This hypothesis is tested by analysing video transects in both ecosystems, assessing megafauna  
28 composition and abundance.

29 Nine video transects (ROV dives) from two different license areas and one Area of Particular  
30 Environmental Interest in the eastern CCZ were analysed. Four of these transects were carried out as  
31 exploratory dives on four different seamounts in order to gain first insights in megafauna  
32 composition. The five other dives were carried out in the neighbouring nodule fields in the same  
33 areas. Variation in community composition observed among and along the video transects was high,  
34 with little morphospecies overlap on intra-ecosystem transects. Despite the observation of  
35 considerable faunal variations within each ecosystem, differences between seamounts and nodule  
36 fields prevailed, showing significantly different species associations characterising them, thus  
37 questioning their use as a possible refuge area.

## 38 1. Introduction

39 Seamounts are abundant and prominent features on the deep-sea floor (Wessel et al., 2010). They  
40 are common in all the world's oceans, occurring in higher abundances around mid-ocean ridges,  
41 island-arc convergent areas, and above upwelling mantle plumes (Kitchingman et al., 2007).  
42 Seamounts are defined as isolated sub-surface topographic feature, usually of volcanic origin, of  
43 significant height above the seafloor (International Seabed Authority (ISA), 2019). They are generally  
44 isolated, typically cone shaped undersea mountains rising relatively steeply at least several hundred  
45 meters from the deep-sea floor. Seamounts comprise a unique deep-sea environment, characterised  
46 by substantially enhanced currents and a fauna that is dominated by suspension feeders, such as  
47 corals (Rogers, 2018). They represent hard substrata in the otherwise soft sediment deep sea and  
48 can thus be considered habitat islands (Beaulieu, 2001). Given the growing evidence that seamounts  
49 differ substantially across a range of spatial scales, the concept of seamounts as a single, relatively  
50 well-defined habitat type is outdated (Clark et al., 2012). Depth and substrate type are key elements  
51 in determining the composition and distribution of benthic fauna on seamounts, while location is  
52 likely the subsequent most important driver of faunal composition and distribution patterns (e.g.  
53 Tittensor et al., 2009). Connectivity varies substantially between seamounts, resulting in the  
54 presence of taxa with very localised to very wide distributions (Clark et al., 2010).

55  
56 The Clarion-Clipperton Fracture Zone (CCZ), in the equatorial eastern Pacific Ocean, is most known  
57 for its extensive polymetallic nodule fields that will potentially be mined in the future. In this area,  
58 nodules represent the most common hard substrate on the soft-sediment abyssal plains, and many  
59 organisms rely on them for survival (Vanreusel et al., 2016). Removal of hard substrate through  
60 mining actions will impact all these organisms, which were estimated at about 50% of all megafaunal  
61 species in the CCZ (Amon et al., 2016). Nodule fields in the CCZ are interspersed by seamounts  
62 (Wedding et al., 2013), the only feature offering hard substrata besides the nodules. Based on this  
63 feature/characteristic, it has been hypothesised that seamounts could provide refuge for organisms  
64 during deep-sea mining activities or that seamounts could play a role in the (re-)colonisation of the  
65 disturbed nodule fields. Whether or not this is true may have important implications for  
66 management of the impacts of polymetallic nodule mining in the CCZ. However, knowledge on the  
67 biodiversity inhabiting seamounts in this region is currently lacking.

68 The objectives of the current study were twofold: (i) Provide first insights in seamount megafauna  
69 within the CCZ, (ii) Compare the benthic fauna inhabiting seamounts and nodule fields in the eastern  
70 CCZ. Since this is the first time the seamounts at the eastern CCZ were visited, a separate section is  
71 dedicated to describe these first insights.

## 72 2. Material and Methods

### 73 2.1. Study site and data

74 During the SO239 ECORESPONSE cruise in 2015 (Martinez Arbizu and Haeckel, 2015), four  
75 seamounts were visited for the first time within two different license areas and one area of  
76 particular environmental interest (APEI) within the Clarion-Clipperton Fracture zone (CCZ) (Table 1).  
77 Nodule fields within the same license areas were visited and sampled as well. Video imagery and  
78 faunal samples were collected by a Remotely Operated Vehicle (ROV Kiel 6000 (GEOMAR), equipped  
79 with a high definition Kongsberg OE14-500 camera).

80 Seamount transects were carried out uphill, towards the summit resulting in a depth gradient along  
81 the transect (Table 1). The four seamount transects were characterised by different depth ranges  
82 and lengths and were, due to the vessel's positioning and the predominant South-East surface  
83 currents, all carried out downstream, on the north to north-western flanks of the seamounts (Table  
84 1 and Fig. 1). The names of the seamounts used here, Rüppel and Senckenberg (BGR, German  
85 License area), Heip (GSR, Belgian License area) and Mann Borgese (APEI3), are the ones agreed upon  
86 by the scientist during the ECORESPONSE cruise (Martinez Arbizu and Haeckel, 2015), pending  
87 incorporation of these names in the GEBCO gazetteer. The seamounts differed in shape and size  
88 with Senckenberg and Heip being a sea-mountain range, while Rüppel and Mann Borgese were more  
89 isolated, stand-alone seamounts (Fig. 1). Nodule field dives were carried out on relatively flat  
90 surfaces (maximum depth range covered during a dive or transect was 30m difference, Table 1) and  
91 were referred to by the dive number and license area. The five nodule transects were all located  
92 between 4000-5000m depth and the transects differed in length between dives as well (Table 1).  
93 Within the same license area, distance between different transects was 16 to 60km, while distance  
94 between license areas added up to several hundreds of kilometres (minimum ~700kms BGR – GSR,  
95 Fig. 1).

96 Investigated areas were restricted to the eastern part of the CCZ with APEI3 being the most north-  
97 and westward bound area. The optical resolution of the camera enabled reliable identification of  
98 organisms larger than 3 cm (Martinez Arbizu and Haeckel, 2015). The combination of exploration  
99 and opportunistic sampling restricted a systematic image collection. Target ROV travelling altitude  
100 was <2m and travelling speed was ~0.2m/s which, along with the camera zoom, were kept constant  
101 whenever possible. Due to the explorative nature of the dives, the pan and tilt of the ROV camera  
102 were not kept constant.

## 103 2.2. Video analysis and statistics

104 All videos were annotated to the lowest taxonomic level possible. The number of morphospecies,  
105 defined as morphologically different organisms within the lowest taxonomic group identified, were  
106 assessed. Identifications were double checked with scientists working in the same area as well as  
107 taxonomic experts and comprise different taxonomic levels (e.g. Genus, Family). Those  
108 identifications restricted to higher taxon groups (Family, Class, etc.) and for which it was impossible  
109 to attribute a morphospecies, were referred to as taxa and are likely to morphologically differ  
110 between transects. Xenophyophores, living on the soft sediment deep-sea floor, were less  
111 prominently present at seamounts than at nodule fields and were not quantified. Fish  
112 (Actinopterygii), Crustacea (Nematocarinidae, Aristeidae, Peracarida) and Polychaeta were  
113 quantified but left out of the comparing statistical analysis due to their lack of representativity and  
114 possible attraction due to ROV lights. The same was done for jellyfish and other doubtful  
115 identifications that could not be confidently assigned to a higher taxonomic group (Table A1). A  
116 subset of the nodule field transects from BGR, GSR and APEI3 was presented by Vanreusel et al.  
117 (2016), corresponding to 44% of what was studied here and limited organism identification to a  
118 higher taxonomic level (Order (e.g. Alcyonacea) or Class (e.g. Ophiuroidea)). In our study, the entire  
119 transects (100%) were annotated to morphospecies level, allowing a detailed comparison between  
120 seamounts and nodule fields.

121 Three categories of substratum types were distinguished: (1) Predominant soft substrata (<40% hard  
122 substrata), (2) mix or transition (between 40 and 60% hard substrata) and (3) predominant hard  
123 substrata (>60% hard substrata), and were annotated per 10m distance units based on the video  
124 footage and tested for correlations with taxonomic abundances.

125 ROV transects on the seamounts were carried out as exploratory dives. Sampling strategy both at  
126 seamounts and nodule fields combined video and sampling or specimen collection. Due to varying  
127 altitude of the ROV and the use of camera pan, tilt and zoom, it was not possible to use surface  
128 coverage as a standardisation measure. We used video transect length instead. For the transect  
129 length calculation for each dive, we omitted all parts of the video footage in which the ROV was at  
130 an altitude of >10m, or sections where the ROV was not visualising the seafloor (e.g. during  
131 transiting or inspecting ROV parts or instruments). Visualisation of ancient disturbance tracks were  
132 omitted as well, as these fell out of the scope of the article. Faunal densities were calculated as the  
133 number of observations per 100m, in order to compensate for time spent collecting samples and  
134 differing transect lengths. Statistical testing was carried out in R (R core team, 2018). Non-metric  
135 multidimensional scaling analysis (NMDS) was based on Bray-Curtis dissimilarity and carried out with  
136 the vegan package (Oksanen et al., 2018). The Kendall's coefficient of concordance (W) was  
137 calculated to identify significantly associated groups of species, based on correlations and  
138 permutations (Legendre, 2005).

### 139 3. Results

140 About 80% of all taxa observed across the two adjacent ecosystems, could be identified to a  
141 morphospecies level. At a first view, morphospecies revealed to be quite different between  
142 seamounts and nodule fields (Fig. 2). While the number of faunal observations at the seamount  
143 transects were within similar ranges (34-42 ind./100m), those at the nodule transects featured both  
144 highest and lowest values (6.3-67.5 ind./100m) (Table 1). The lowest number of faunal observations  
145 were done at the two APEI3 nodule transects (ROV13 and 14) and highest at the GSR nodule  
146 transect ROV10. What follows is a first description of eastern CCZ seamount megafauna (3.1.) and a  
147 detailed comparison with the neighbouring nodule fields (3.2.)

#### 148 3.1. Insights in CCZ seamount megafauna

149 The most abundant and diverse (most morphospecies) taxa at the seamount transects comprised  
150 Echinodermata (Asteroidea, Crinoidea, Holothuroidea and Ophiuroidea), Anthozoa (Actiniaria,  
151 Alcyonacea, Pennatulacea, Scleractinia) and Porifera (Hexactinellida) (Table A1, Fig. 3). Keeping in  
152 mind the limitation of the video sampling, differences among the benthic seamount community  
153 composition are described here. The transect at Mann Borgese (APEI3) was characterised by high  
154 densities of Antipatharia, more specifically Antipathidae (18.5 ind./100m), and solitary Scleractinia  
155 (7.9 ind./100m) (Table A1, Fig. 3). Antipathidae observations were mostly grouped at the end of the  
156 video transect, i.e. at the summit. Densities of both Antipatharia and Scleractinia were much lower  
157 on the other seamount transects (<1 ind./100m) with Scleractinia being absent from Heip and  
158 Senckenberg transects. Alcyonacea corals were observed on all seamount transects. Isididae were  
159 found at Senckenberg and Heip transects, and one individual from the Chrysogorgiidae family was  
160 observed at the latter as well. Varying numbers of Primnoidae were observed on all transects (Table  
161 A1). High abundances of Pennatulacea were observed at Senckenberg (3.8 ind./100m), representing  
162 about 28% of sessile fauna annotations for this transect.

163 Enteropneusta were only observed on Rppel and Senckenberg transects in the BGR area,  
164 represented by two different morphospecies, namely *Yoda* morphospecies (Torquaratoridae) at  
165 Rppel and *Saxipendium* morphospecies (Harrimaniidae) at Senckenberg.

166 Highest Polychaeta densities were observed at Heip transect in the GSR area, which was mainly due  
167 to high densities of free-swimming Acrocirridae (4.2 ind./100m vs. 0.2 ind./100m in BGR area Table  
168 A1). Aphroditidae polychaetes were only present at the BGR transects (0.2 ind./100m  
169 (corresponding to 3 individuals along the transect) at Rppel and 0.04 ind/100m (or 1 individual along  
170 the transect) at Senckenberg) (Table A1).

171 Porifera densities were highest at the Heip transect (7.5 ind./100m), followed by Rppel  
172 (3.5 ind./100m), Senckenberg (1.9 ind./100m) and lastly Mann Borgese (1.8 ind./100m). Six Porifera  
173 families were annotated featuring >7 to >10 morphospecies (Fig. 3, Table A1). Cladorhizidae (two  
174 individuals) were only observed on Heip transect, and one *Poliopogon* sp. (Pheronematidae) was  
175 observed at Mann Borgese transect. Rossellidae gen. sp. nov. was present on three seamount  
176 transects, exception being Mann Borgese.

177 Overall Echinodermata densities were highest at Senckenberg seamount (17 ind./100m), followed by  
178 Rppel (10 ind./100m) (Table A1, Fig. 3), both adding up to 47% of all image annotations for these  
179 transects. The number of morphospecies for all echinoderm taxa (Asterozoa, Echinozoa,  
180 Holothurozoa and Crinozoa) was also highest at these 2 seamounts in the BGR area (Fig. 3). For  
181 comparison, echinoderms at Heip (10 ind./100m) and Mann Borgese transects (3.3 ind./100m) were  
182 responsible for 32% and 8.2% of observations respectively. Crinozoa densities were highest at  
183 Senckenberg (4.2 ind./100m), while Holothurozoa were most abundant at Rppel (4.4 ind./100m).  
184 The holothuroid families of Elpidiidae and Laetmogonidae were only observed at Senckenberg and  
185 Rppel (BGR). Psychropotidae and Synallactidae were observed on all seamounts, represented by  
186 different morphospecies. Deimatidae were not observed on Mann Borgese, but were present on the  
187 three other seamount transects, again with different morphospecies and densities. Velatid  
188 Asterozoa were only observed at Senckenberg and Rppel (BGR), while Brisingida and Paxillosida  
189 were observed on all four seamounts. Aspidodiadematid Echinozoa were absent from the Heip  
190 transect and urchinid Echinozoa were absent from the Mann Borgese transect.

191 A species accumulation curve (Fig. 4a) confirmed the limitations of the restricted and exploratory  
192 nature of the sampling as no asymptote was reached. The rarefaction curves (Fig. 4b) showed that  
193 the transects with the most faunal observations, which corresponded here to the longer transects,  
194 were more diverse. However, at smaller sample sizes curves did not cross, thus maintaining the  
195 differences observed at higher sample sizes with the Senckenberg transect (ROV04) as most diverse  
196 followed by Rppel (ROV02) (both BGR). The video transect carried out at Mann Borgese (ROV15,  
197 APEI3) was the least diverse.

198 A comparison of all morphospecies observed along the 4 transects was presented in a Venn diagram  
199 (Fig. 5a). Each seamount transect was characterised by a highest number of unique morphospecies,  
200 only observed on the transect in question and not elsewhere. Only three morphospecies were  
201 present in all seamount transects, namely *Ceriantharia* msp. 2, a small red galatheid crab and a  
202 foliose sponge. Highest number of overlapping morphospecies (#16) was observed between Rppel

203 and Senckenberg, both in the BGR area (Fig. 5a). Mann Borgese showed the smallest degree of  
204 overlap with the other transects (Fig. 5a).

205  
206 About 57% of all sessile fauna was associated with predominantly hard substrata, followed by 31%  
207 on the mixed substrata. For the mobile taxa, the pattern was less pronounced with 41 and 42%  
208 associated with predominantly hard and mixed hard/soft substrata respectively. The amount of  
209 predominantly hard and soft substrata was negatively correlated, though not significantly. This was  
210 due to the equal amounts (40-60%) of mixed hard/soft substrata. Over all seamount transects  
211 pooled together, no taxa were significantly correlated with the amount of hard substrata, nor with  
212 soft substrata. When looking at the individual transects, no significant correlations were found  
213 between taxa and substrata for ROV02 or ROV04 or ROV09, most likely due to the equal distribution  
214 of the amount of hard/soft/mix substrata. In this perspective, ROV15 stood out, as it was dominated  
215 by predominantly hard substrata (56%). For this transect, Pennatulacea were significantly  
216 negatively correlated with the amount of hard substrata and Zoantharia/Octocorralia were  
217 significantly and positively correlated with hard substrata, as were Ophiuroidea, Asteroidea,  
218 Crinoidea and Mollusca.

219  
220 Due to the limited sample size, the representativity of the observed biological patterns remains to  
221 be corroborated by a more elaborate sampling strategy.

### 222 3.2. Comparison of seamount and nodule field faunal composition and variation

223 The faunal composition and richness (number of morphospecies in higher taxonomic groups) of the  
224 nodule transects can be consulted in Fig. 3 and Table A1, respectively. In concordance with the  
225 seamount transect, the species accumulation curve of the nodule transects did not reach an  
226 asymptote either (Fig. 4c). The rarefaction curves showed that the relations among transects were  
227 less straightforward for the nodule transects versus the seamount ones and did cross at smaller  
228 sample sizes (<100 individuals, Fig. 4d). ROV13 and ROV14 transects (both APEI3) were the longest in  
229 distance travelled (Table 1) but featured less faunal observations. At small sample sizes, the richness  
230 at ROV13 and 14 was highest. ROV08 and ROV10 (both GSR) showed parallel curves with ROV08  
231 being more diverse (Fig. 4d).

232 A venn diagram showing the morphospecies overlap among the nodule transects showed a total of 5  
233 species re-occurring on all 5 transects (Fig. 5b). These were: Munnopsidae msp. 1 (Isopoda,  
234 Crustacea), Actiniaria msp.7 (Cnidaria), Ophiuroidea msp. 6 (Echinodermata), *Holascus* sp. and  
235 *Hyalonema* sp. (Hexactinellida, Porifera). There was a high number of unique morphospecies for  
236 each transect, though not as high as for the seamount transects (Fig. 5). ROV13 and 14 (both APEI3)  
237 showed least overlap with the other transects, which is similar to what was observed at the  
238 seamounts.

239 Observations and quantifications of morphospecies confirmed the high degree of dissimilarity  
240 between the two neighbouring ecosystems. Porifera, Ophiuroidea (Echinodermata), Actiniaria and  
241 Alcyonacea (Cnidaria) were more abundant at nodule fields (Fig. 3). These taxonomic groups were  
242 also most diverse on nodule fields (i.e. highest number of morphospecies), exception being the  
243 Alcyonacea which featured more morphospecies on the seamounts (12 to 8 morphospecies for  
244 seamounts and nodule fields respectively) (Fig. 3). Of all Porifera, Cladhorizidae were more diverse  
245 at nodule fields than at seamounts (7 to 1 morphospecies, respectively).

246 There were only 21 morphospecies (10%) that were observed both on seamounts and nodule fields  
247 (Fig. 6). While this subset of morphospecies occurred in both ecosystems, they did so in very  
248 different densities, i.e. very abundant in one ecosystem and very low in abundance in the other:  
249 examples are Galatheidae small red msp. (Decapoda, Crustacea), *Synallactes* white msp.  
250 (Holothuroidea), Ophiuroidea msp. 5 and 6, Comatulida msp. 1 (Crinoidea), *Hyalonema* sp. and  
251 *Hyalostylus* sp. (both Hexactinellida, Porifera) (Fig. 6).

252 Three Ophiuroidea morphospecies were present at both seamounts and nodule fields (Fig. 2, 3 and  
253 6). The majority of the very abundant Ophiuroidea observed at the CCZ seamounts were small and  
254 situated on hard substrata (morphospecies 5), while most of the Ophiuroidea at nodule fields  
255 (including morphospecies 6) were observed on the soft sediments. Morphospecies 6 was only rarely  
256 observed on the seamounts (Fig. 3). Another easily recognisable morphospecies was found on  
257 Porifera, coral and animal stalks and was more abundant at seamounts than at nodule fields  
258 (morphospecies 4) (Fig. 2 and 3).

259 Crinoidea, Asteroidea (both Echinodermata) and Antipatharia (Cnidaria) were more abundant on the  
260 seamounts (Fig. A1). This coincided with a higher diversity for Asteroidea and Antipatharia on the  
261 seamounts as well. Crinoidea diversity was similar (5 to 4 morphospecies comparing seamounts to  
262 nodule fields). Holothuroidea occurred in similar densities in both ecosystems (Fig. A1, though they  
263 were characterised by different morphospecies (Fig. 3). Overall densities of Echinoidea were  
264 comparable between seamounts and nodule fields, though for the nodule fields this was mostly due  
265 to one very abundant morphospecies, namely Aspidodiadematidae msp 1, which was absent at the  
266 seamounts (Fig. 3). Besides this, Echinoidea were more diverse at seamounts (11 morphospecies vs.  
267 5 at nodule fields).

268 There was no morphospecies overlap for Tunicata, Antipatharia, and Actiniaria. Alcyonacea,  
269 Ceriantharia, Corallimorphidae and Crinoidea only shared 1 morphospecies between seamounts and  
270 nodule fields, namely *Callozostron* cf. *bayeri*, Ceriantharia msp. 2, *Corallimorphus* msp. 2 and  
271 Comatulida msp. 1 respectively (Fig. 6).

272 There were no observations of Enteropneusta, Scleractinia and Zoantharia (Cnidaria), Aphroditidae  
273 (Polychaeta) or holothuroid Deimatidae at the nodule fields transects (Table A1, Fig. A1). While  
274 Actinopterygii were left out of the analysis, it should be noted that fish observations were more  
275 diverse at the seamounts than on the nodule fields.

276 There was quite some faunal variation observed among the video transects of, both seamounts and  
277 nodule fields (see Fig. 5). The (dis)similarities were analysed by a nMDS analysis, which grouped the  
278 9 different video transects based on their taxonomic composition. Despite the large intra-ecosystem  
279 variation, they pooled in two distinct groups separating the nodule fields from the seamounts (Fig.  
280 7a). Within each group, BSR and GSR transects were more similar to one another both for  
281 seamounts and nodule fields, whilst APEI3 transects stood out more.

282 The Kendall's coefficient of concordance ( $W$ , Legendre, 2005) corroborated the existence of two  
283 significantly different species associations, whose composition corresponded to the fauna  
284 characterising the nodule fields ( $W=0.20$ ,  $p<0.001$ , after 999 permutations) and the seamounts  
285 ( $W=0.30$ ,  $p<0.001$ , after 999 permutations).

286 Depth was fitted as a vector on top of the nMDS plot (Fig. 7b) and showed that the discrepancy in  
287 faunal composition between the two ecosystems also corresponded to a difference in depth, with  
288 the nodule transects all being situated below the 4000m isobath and the seamount transects ranging  
289 from 1650 to >3500m (Fig. 7b).

## 290 4. Discussion

### 291 4.1. Intra-ecosystem faunal variation

292 Community composition varied markedly at seamounts and nodule fields. The limited sampling (n=9  
293 transects), at different locations and additionally, for the seamounts, different depth ranges,  
294 precluded any general conclusions on quantifications of biodiversity *per se*. However, taking this into  
295 account, it was also the first time seamounts were visited in the area, thus granting first insights in  
296 the fauna inhabiting these seamounts and allowing a first comparison with nodule faunal  
297 composition.

298 The two BGR seamount transects were most similar in faunal composition, followed by the Heip  
299 seamount transect (GSR). These seamount video transects were characterised by more similar depth  
300 ranges, and the two BGR transects were also geographically closest to each other. Although for  
301 seamounts, distance separating them might be a less determining factor than depth since  
302 (mega)faunal communities can be very different even between adjacent seamounts (Schlacher et al.,  
303 2014; Boschen et al., 2015). Overall, parameters that vary with depth, such as temperature, oxygen  
304 concentration, substratum type, food availability, and pressure are considered major drivers of  
305 species composition on seamounts (Clark et al., 2010; McClain et al., 2010). The quantification of the  
306 amount of hard and soft substrata was not distinctive enough to explain differences observed here.  
307 The difference in depth could also explain the higher dissimilarity with Mann Borgese (APEI3) who  
308 featured the shallowest transect and summit, which was dominated by Antipatharia. Antipatharians  
309 were previously reported to be more dominant towards peaks as compared to mid-slopes at  
310 corresponding depths (Genin et al., 1986). Based on their filter-feeding strategy, Porifera (except  
311 carnivorous Cladorhizidae), were also thought to benefit from elevated topography (peaks) or  
312 exposed substrata in analogy to corals (Genin et al., 1986; Clark et al., 2010), though no such pattern  
313 was apparent here. Porifera are notoriously difficult to identify based on imagery. Although the  
314 sampled individuals allowed some identifications to genus or species level (Kersken et al., 2018a and  
315 b), identifications remained hard to extrapolate across the different video transects. Generally, as in  
316 our study, seamount summits have been more intensively sampled (Stocks, 2009) although the little  
317 work done at seamount bases and deep slopes indicated that these areas support distinct  
318 assemblages (Baco, 2007).

319 Among the nodule transects a considerable amount of variation in faunal composition was observed  
320 (this study, Vanreusel et al., 2016). The two APEI3 nodule transects (ROV13 and 14) stood out in  
321 faunal composition, diversity and in low number of faunal observations. They were also the only two  
322 transects situated below the 4500m isobaths. But rather than depth, the nodule coverage may be  
323 considered an important driving factor, since the density of nodule megafauna was shown to vary  
324 with nodule size and density/coverage (Stoyanova, 2012; Vanreusel et al., 2016, Simon-Llédó et al.,  
325 2019). Here as well, the APEI3 transects were characterised by a high nodule coverage (~40-88%,  
326 Vanreusel et al., 2016), whereas the BGR and GSR nodule transects (ROV3 and ROV 8 + 10,  
327 respectively) had a nodule coverage <30% and were also more similar in faunal composition  
328 (Vanreusel et al., 2016). Other factors that could be at play are the more oligotrophic surface waters



329 of the northern CCZ which could be the cause of the overall lower faunal densities at APEI3 nodule  
330 fields (Vanreusel et al., 2016). Volz et al. (2018) corroborated this, with the location of the APEI3 site  
331 in the proximity of the carbon-starved North Pacific gyre being characterised by a reduced POC-flux  
332 quantified to being 22-46% lower than the GSR and BGR areas respectively.

333 The species accumulation curves showed that no asymptote was reached neither at seamounts, nor  
334 at nodule fields. Consequently, longer transect lengths might be necessary to representatively  
335 quantify and assess megafauna density and diversity (Simon-Lledó et al., 2019). In addition, for a first  
336 in-depth description and assessment of seamount fauna composition, one video transect is  
337 insufficient to describe the diversity and shifts in faunal assemblages of the surveyed seamounts.  
338 Rather, an ampler imaging strategy should be developed, with a minimum transect length exceeding  
339 1000ms (Simon-Lledó et al., 2019) and replicate transects carried out on different faces of the  
340 seamount, on slopes with varying degree of exposure to currents and different substrate types.  
341 Wider depth ranges should be taken into account as well. Alternatively, across slope transects,  
342 following depth contours should be considered as these could provide observation replicates for a  
343 given depth. Despite its limitations, this study grants first insights in the seamount inhabiting  
344 megafauna of the eastern CCZ and an important first comparison with nodule fauna.

#### 345 4.2. Faunal (dis)similarities between seamounts and nodule fields

346 In other areas, seamounts were shown to share fauna with surrounding habitats (Clark et al., 2010)  
347 and could thus potentially serve as source populations for neighbouring environments (McClain et  
348 al., 2009). While generally few species seemed restricted to seamounts only (Clark et al., 2010),  
349 morphospecies in this study revealed to be quite different between seamounts and nodule fields  
350 with little overlap between both. Despite the high degree of variation observed among all the video  
351 transects, these grouped into two distinctly separate clusters, separating nodule from seamount  
352 transects. The few overlapping morphospecies did occur in different densities in each ecosystem,  
353 implying a different role or importance in the ecological community and its functioning.

354 Overall, nodule fields showed higher faunal densities than seamounts. Shifts in density patterns  
355 between nodule fields and seamounts were more evident in a number of taxa, where the variety of  
356 morphospecies and feeding strategy within each group was likely to be at play. An example of this  
357 are the Echinodermata, which include Asteroidea (predators and filter feeders (Brisingida)),  
358 Crinoidea (filter feeders), Echinoidea (deposit feeders), Holothuroidea (deposit feeders) and  
359 Ophiuroidea (omnivores). Asteroidea were more abundant on seamounts and both Echinoidea and  
360 Asteroidea were more diverse in this ecosystem as well. Ophiuroidea were most abundant on the  
361 nodule fields (ratio 7 to 1 when compared to seamounts). Same ophiuroid morphospecies were  
362 present at seamounts and nodule fields but in very different abundances and they were observed on  
363 different substrata types, which indicates different lifestyles, feeding behaviour and corresponding  
364 dietary specialisations (Persons and Gage, 1984). Previously it was already demonstrated that  
365 Ophiuroidea did not show high levels of richness or endemism on seamounts (O'Hara, 2007). At  
366 nodule fields, Ophiuroidea were often observed in association with xenophyophores (Amon et al.,  
367 2016, this study) and a similar observation was done at east Pacific seamounts off Mexico (Levin et  
368 al., 1986), though no such associations were observed on the seamounts studied here.

369 Holothuroidea densities were thought to possibly decrease when less soft sediment was available  
370 since they feed mainly on the upper layers of the soft-bottom sediment (Bluhm and Gebruk, 1999).

371 No significant link was established between holothuroid densities and the amount of hard substrata  
372 in this study, but their community composition varied distinctly between nodule fields and  
373 seamounts with more families being observed at the latter. Additionally, at the seamounts, many  
374 holothurians were observed on top of rocks, possibly reflecting different feeding strategies and  
375 explaining the observations of different morphospecies. Geographical variations, different bottom  
376 topography, differences in nodule coverages and sizes and/or an uneven distribution of holothurians  
377 on the sea floor were thought to play a role in holothuroid community composition (Bluhm and  
378 Gebruk, 1999). On the other hand, variability in deep-sea holothuroid abundance was proposed to  
379 depend primarily on depth and distance from continents (see Billet, 1991 for a review).

380 Stalked organisms, such as Crinoidea (Echinodermata) and Hexactinellida (except for  
381 Amphidiscophora, Porifera) rely on hard substrata for their attachment and are considered being  
382 among the most vulnerable organisms when mining is concerned. Crinoidea were more abundant on  
383 seamounts, possibly because hard substrata were less limiting than in the nodule fields. Porifera  
384 densities (stalked and non-stalked) varied among all analysed transects, revealing no particular  
385 trends in abundance. However, the species composition of deep-sea glass sponge communities from  
386 seamounts and polymetallic nodule fields was distinctly different. Polymetallic nodule field  
387 communities were dominated by widely-distributed genera such as *Caulophacus* and *Hyalonema*,  
388 whereas seamount communities seemed to have a rather unique composition represented by  
389 genera like *Saccocalyx*.

390 Corals were generally considered to be more abundant on seamounts than adjacent areas, due to  
391 their ability to feed on a variety of planktonic or detritus sources suspended in the water column  
392 (Rowden et al., 2010). In this study, the Alcyonacea densities were lower on the seamounts than on  
393 the nodule transects. The majority of Alcyonacea morphospecies of the seamounts did not occur on  
394 the nodule fields and vice versa, with exception of *Callozostron cf. bayeri* which was also present at  
395 the nodule fields but in very low densities (1/10 of those observed at seamounts). The Antipatharia  
396 were most abundant at the Mann Borgese seamount (APEI3) compared to all other transects. The  
397 depth difference of more than 3000m between this particular seamount and the nodule fields could  
398 explain the abundance in Antipatharia which were shown to be more abundant at lower depths  
399 (Genin et al., 1986). Additional presence of Pennatulacea at seamounts, a taxon that was virtually  
400 absent from the nodule field transects and that appeared more linked to predominant soft substrata  
401 at seamounts, resulted in completely distinct coral communities for each ecosystem.

402 Actiniaria were denominated the second most common group at CCZ nodule fields, after the  
403 xenophyophores (Kamenskaya et al., 2015) and, in our study, were also more abundant on nodule  
404 fields than on seamounts. Depending on the species and feeding strategy, the ratio hard/soft  
405 substrata and their preference for either one could play a role. Since morphospecies were distinct  
406 between seamounts and nodule fields, their role in the respective communities are likely to differ as  
407 well. Combinations of deposit feeding and predatory behaviour in Actiniaria have been observed, as  
408 well as burrowing activity, preference for attachment to hard substrata and exposure to currents  
409 (Durden et al., 2015a; Lampitt and Paterson, 1987; Riemann-Zürneck, 1998), all factors that could  
410 influence the differences in morphospecies observed.

411 Some taxa were only observed on the seamounts in this study, while they occurred on nodule fields  
412 elsewhere, be it in low densities. For instance, Enteropneusta, which in this study were found only

413 on seamounts, were observed previously at CCZ nodule fields though observations were rather rare  
414 (Tilot, 2006). They appeared more abundant at the nodule fields of the Deep Peru Basin (DISCOL  
415 area), though a wide range in abundances was displayed there as well (Bluhm, 2001). The exception  
416 were the Scleractinia, which were quite common on seamounts, as also reported in other studies  
417 (e.g. Baco, 2007, Rowden et al., 2010), but distinctly absent at nodule fields.

418 Explanation for the discrepancies in faunal composition and the low degree of morphospecies  
419 overlap between seamount and nodule fields, as observed here, can be multiple. For one, nodules  
420 may not be considered a plain hard substratum, with their metal composition, microbial colonisation  
421 and the nodule/sediment interface influencing the epi- and associated megafaunal composition. The  
422 possibility of a specific deep-sea faunal community that tolerates or benefits from manganese  
423 substrata has been previously proposed (Mullineaux, 1988). The comparison between seamounts  
424 and nodule fields as two neighbouring hard-substrata ecosystems also entailed a comparison  
425 between depth gradients and possible thresholds (>4000m for nodule fields and 1500 < x < 4000m for  
426 seamounts). Related to this is the steepness of the seamount slope and its current exposure playing  
427 a role in the faunal colonisation (Genin et al., 1986; Rappaport et al., 1997). Other studies showed  
428 that habitat heterogeneity increased megafaunal diversity at seamounts (Raymore, 1982) and  
429 elsewhere, such as abyssal plains (Lapointe and Bourget, 1999; Durden et al., 2015b, Leitner et al.,  
430 2017, Simon-Llédo et al., 2019). Within this perspective the smaller-scale substratum heterogeneity  
431 transcending the ratio hard/soft substrata or amount of hard substrata could play a role as well.

## 432 5. Conclusions

433 Based on our current knowledge; seamounts appear inadequate as refuge areas to help maintain  
434 nodule biodiversity. In order to conclusively exclude seamount habitats as a refuge for nodule fauna,  
435 a more comprehensive sampling should be carried out. The sampling strategy wielded in this study  
436 lacked replicates, uniformity and was limited in sample size. Seamount bases should be taken into  
437 consideration as well as they can be characterised by distinctly different assemblages than the  
438 summits and they feature depth ranges more similar to nodule fields.

439 While their role as refuge area for nodule field fauna is currently debatable, the possible uniqueness  
440 of the seamount habitat and its inhabiting fauna implies that seamounts need to be included in  
441 management plans for the conservation of the biodiversity and ecosystems of the CCZ.

## 442 Author Contributions

443 DC, PAR, SPR, DK analysed the images. DC analysed the data. PMA, PAR, AC conceptualised and  
444 carried out the sampling. All authors contributed to the redaction of the manuscript.

## 445 Data Availability

446 Data sets are made available through OSIS-Kiel data portal, BIIGLE and PANGAEA.

## 447 Competing interest

448 The authors declare that they have no conflict of interest

## 449 Acknowledgments

450 We thank the crew of SO239 and GEOMAR for their support in acquiring the images used in this  
451 article. The EcoResponse cruise with RV Sonne was financed by the German Ministry of Education  
452 and Science BMBF as a contribution to the European project JPI-Oceans “Ecological Aspects of Deep-  
453 Sea Mining”. This study had the support of PO AÇORES 2020 project Acores-01-0145-Feder-  
454 000054\_RECO and of Fundação para a Ciência e Tecnologia (FCT), through the strategic projects  
455 UID/MAR/04292/2013 granted to MARE. The authors acknowledge funding from the JPI Oceans—  
456 Ecological Aspects of Deep Sea Mining project by Fundação para a Ciência e Tecnologia de Portugal  
457 (Mining2/0005/2017) and the European Union Seventh Framework Programme (FP7/2007–2013)  
458 under the MIDAS project, grant agreement n° 603418. DC is supported by a post-doctoral  
459 scholarship (SFRH/BPD/110278/2015) from FCT. PAR was funded by the Portuguese Foundation for  
460 Science and Technology (FCT), through a postdoctoral grant (ref. SFRH/BPD/69232/2010) funded  
461 through QREN and COMPETE. SPR is supported by FCT in the scope of the “CEEC Individual 2017”  
462 contract (CEECIND/00758/2017) and CESAM funds (UID/AMB/50017/2019) through FCT/MCTES. AC  
463 is supported by Program Investigador (IF/00029/2014/CP1230/CT0002) from FCT. PMA  
464 acknowledges funding from BMBF contract 03 F0707E. Pictures were provided by GEOMAR (Kiel).  
465

## 466 References

- 467 Amon, D. J., Ziegler, A. F., Dahlgren, T. G., Glover, A. G., Goineau, A., Gooday, A. J., Wiklund, H.,  
468 and Smith, C. R.: Insights into the abundance and diversity of abyssal megafauna in a  
469 polymetallic-nodule region in the eastern Clarion-Clipperton Zone. *Sci. Rep.*, 6(1), 30492.  
470 <https://doi.org/10.1038/srep30492>, 2016
- 471 Baco, A.R. : Exploration for deep-sea corals on North Pacific seamounts and islands. *Oceanography*  
472 20:109– 17, 2007
- 473 Beaulieu, S. E.: Colonization of habitat islands in the deep sea: Recruitment to glass sponge stalks.  
474 *Deep-Sea Res Pt I*, 48(4), 1121–1137. [https://doi.org/10.1016/S0967-0637\(00\)00055-8](https://doi.org/10.1016/S0967-0637(00)00055-8), 2001
- 475 Bluhm, H.: Re-establishment of an abyssal megabenthic community after experimental physical  
476 disturbance of the seafloor. *Deep-Sea Res Pt II*, 48(17–18), 3841–3868.  
477 [https://doi.org/10.1016/S0967-0645\(01\)00070-4](https://doi.org/10.1016/S0967-0645(01)00070-4), 2001
- 478 Bluhm, H., and Gebruk, A. V.: Holothuroidea (Echinodermata) of the Peru basin - ecological and  
479 taxonomic remarks based on underwater images. *Mar. Ecol.*, 20(2), 167–195.  
480 <https://doi.org/10.1046/j.1439-0485.1999.00072.x>, 1999
- 481 Boschen, R. E., Rowden, A. A., Clark, M. R., Barton, S., Pallentin, A., and Gardner, J.: Megabenthic  
482 assemblage structure on three New Zealand seamounts: implications for seafloor massive sulfide  
483 mining. *Mar. Ecol. Prog. Ser.*, 523, 1–14. <https://doi.org/10.3354/meps11239>, 2015
- 484 Clark, M. R., Rowden, A. A., Schlacher, T., Williams, A., Consalvey, M., Stocks, K. I., Rogers, A.D.,  
485 O’Hara, T.D., White, M., Shank, T.M., and Hall-Spencer, J. M.: The Ecology of Seamounts:  
486 Structure, Function, and Human Impacts. *Annu. Rev. Mar. Sci.*, 2(1), 253–278.  
487 <https://doi.org/10.1146/annurev-marine-120308-081109>, 2010
- 488 Clark, M.R., Schlacher, T.A., Rowden, A.A., K. Stocks, K.I., and Consalvey, M.: Science priorities  
489 for seamounts: research links to conservation and management. *PLoS One* 7(1): e29232., 2012
- 490 Durden, J. M., Bett, B. J., and Ruhl, H. A.: The hemisessile lifestyle and feeding strategies of *Iosactis*  
491 *vagabunda* (Actiniaria, Iosactiidae), a dominant megafaunal species of the Porcupine Abyssal  
492 Plain. *Deep-Sea Res Pt I* 102, 72–77. <https://doi.org/10.1016/j.dsr.2015.04.010>, 2015a
- 493 Durden, J. M., Bett, B. J., Jones, D. O. B., Huvenne, V. A. I., and Ruhl, H. A.: Abyssal hills - hidden  
494 source of increased habitat heterogeneity, benthic megafaunal biomass and diversity in the deep  
495 sea. *Prog. Oceanogr.*, 137, 209–218, <https://doi.org/10.1016/j.pocean.2015.06.006>, 2015b
- 496 Genin, A., Dayton, P. K., Lonsdale, P., and Spiess, F. N.: Corals on seamount peaks provide evidence  
497 of current acceleration over deep-sea topography. *Nature*, 322, 59–61, 1986

498 International Seabed Authority (ISA): <https://www.isa.org/jm/scientific-glossary/>, last access: 29  
499 October 2019

500 Kamenskaya, O. E., Gooday, A. J., Tendal, O. S., and Melnik, V. F.: Xenophyophores (Protista,  
501 Foraminifera) from the Clarion-Clipperton Fracture Zone with description of three new species.  
502 *Mar. Biodivers.*, 45(3), 581–593. <https://doi.org/10.1007/s12526-015-0330-z>, 2015

503 Kersken, D., Janussen, D., and Martinez Arbizu, P.: Deep-sea glass sponges (Hexactinellida) from  
504 polymetallic nodule fields in the Clarion-Clipperton Fracture Zone (CCFZ), northeastern  
505 Pacific: Part I – Amphidiscophora. *Mar. Biodivers.* 48, 545–573. <https://doi.org/10.1007/s10750-017-3498-3>, 2018a

507 Kersken, D., Janussen, D., and Martinez Arbizu, P.: Deep-sea glass sponges (Hexactinellida) from  
508 polymetallic nodule fields in the Clarion-Clipperton Fracture Zone (CCFZ), northeastern  
509 Pacific: Part II—Hexasterophora. *Mar. Biodivers.* <https://doi.org/https://doi.org/10.1007/s12526-018-0880-y>, 2018b

511 Lampitt, R. S., and Paterson, G. L. J.: The feeding behaviour of an abyssal sea anemone from in situ  
512 time lapse photographs and trawl samples. *Oceanol. Acta*, 10(4), 455–461, 1987

513 Lapointe, L., and Bourget, E.: Influence of substratum heterogeneity scales and complexity on a  
514 temperate epibenthic marine community. *Mar. Ecol. Prog. Ser.*, 189(2), 159–170.  
515 <https://doi.org/10.3354/meps189159>, 1999

516 Leitner, A. B., Neuheimer, A. B., Donlon, E., Smith, C. R., and Drazen, J. C.: Environmental and  
517 bathymetric influences on abyssal bait-attending communities of the Clarion Clipperton Zone.  
518 *Deep-Sea Res Pt I*, 125, 65–80. <https://doi.org/10.1016/j.dsr.2017.04.017>, 2017

519 Levin, L., DeMaster, D., McCann, L., and Thomas, C.: Effects of giant protozoans (class:  
520 Xenophyophorea) on deep-seamount benthos. *Mar. Ecol. Prog. Ser.*, 29, 99–104.  
521 <https://doi.org/10.3354/meps029099>, 1986

522 McClain, C. R., Lundsten, L., Barry, J., and DeVogelaere, A.: Assemblage structure, but not diversity  
523 or density, change with depth on a northeast Pacific seamount. *Mar. Ecol.*, 31, 14–25.  
524 <https://doi.org/10.1111/j.1439-0485.2010.00367.x>, 2010

525 McClain, C. R., Lundsten, L., Ream, M., Barry, J., and DeVogelaere, A.: Endemicity, biogeography,  
526 composition, and community structure on a Northeast Pacific seamount. *PLoS ONE*, 4(1).  
527 <https://doi.org/10.1371/journal.pone.0004141>, 2009

528 Mullineaux, L.S.: The role of settlement in structuring a hard-substratum community in the  
529 deep sea. *J. Exp. Mar. Biol. Ecol.* 120, 241–261, 1988

530 O’Hara, T. D.: Seamounts: Centres of endemism or species richness for ophiuroids? *Glob. Ecol.*  
531 *Biogeogr.*, 16(6), 720–732. <https://doi.org/10.1111/j.1466-8238.2007.00329.x>, 2007

532 Oksanen, J., Blanchet, G., Friendly, M., Kindt, R., Legendre, P., McGlenn, D., Minchin, P.R., O’Hara,  
533 R.B., Simpson, G.L., Solymos, P., Stevens, M.H.H., Szoecs, E., and Wagner, H.: *vegan*:  
534 *Community Ecology Package*. R package version 2.5-2. [https://CRAN.R-  
535 project.org/package=vegan](https://CRAN.R-project.org/package=vegan), 2018

536 Rappaport, Y., Naar, D. F., Barton, C. C., Liu, Z. J., and Hey, R. N.: Morphology and distribution of  
537 seamounts surrounding Easter Island. *J. Geophys. Res.*, 102(B11), 24713.  
538 <https://doi.org/10.1029/97JB01634>, 1997

539 R Core Team: *R: A language and environment for statistical computing*. R Foundation for Statistical  
540 Computing, Vienna, Austria. URL <https://www.R-project.org/>, 2018

541 Riemann-Zürneck, K.: How sessile are sea anemones? A review of free-living forms in the Actiniaria  
542 (Cnidaria: Anthozoa). *Mar. Ecol.*, 19(4), 247–261. <https://doi.org/10.1111/j.1439-0485.1998.tb00466.x>, 1998

544 Rogers, A.D.: The Biology of Seamounts: 25 years on. *Adv. Mar. Biol.* 79, 137–224,  
545 <https://doi.org/10.1016/bs.amb.2018.06.001>, 2018

546 Rowden, A.A., Schlacher, T.A., Williams, A., Clark, M.R., Stewart, R., Althaus, F., Bowden, D.A.,  
547 Consalvey, M., Robinson, W. and Dowdney, J.: A test of the seamount oasis hypothesis:  
548 seamounts support higher epibenthic megafaunal biomass than adjacent slopes. *Mar Ecol*, 31,  
549 95–106, <https://doi.org/10.1111/j.1439-0485.2010.00369.x>, 2010

550 Simon-Iledó, E., Bett, B. J., Huvenne, V. A. I., Schoening, T., Benoist, N. M. A., Je, R. M., Durden,  
551 J.M, and Jones, D. O. B.: Megafaunal variation in the abyssal landscape of the Clarion  
552 Clipperton Zone, *Progr. Oceanogr.* 170, 119–133. <https://doi.org/10.1016/j.pocean.2018.11.003>,  
553 2019

554 Tilot, V., Ormond, R., Moreno Navas, J., and Catalá, T. S.: The Benthic Megafaunal Assemblages of  
555 the CCZ (Eastern Pacific) and an Approach to their Management in the Face of Threatened  
556 Anthropogenic Impacts. *Front Mar Sci.*, 5, 1–25. <https://doi.org/10.3389/fmars.2018.00007>,  
557 2018

558 Vanreusel, A., Hilario, A., Ribeiro, P. A., Menot, L., and Arbizu, P. M.: Threatened by mining,  
559 polymetallic nodules are required to preserve abyssal epifauna. *Sci. Rep.*, 6(1), 26808.  
560 <https://doi.org/10.1038/srep26808>, 2016

561 Wedding, L. M., Friedlander, A. M., Kittinger, J. N., Watling, L., Gaines, S. D., Bennett, M., Hardy,  
562 S.M., and Smith, C.R.: From principles to practice : a spatial approach to systematic  
563 conservation planning in the deep sea. *Proc. R. Soc. B* 280: 20131684.  
564 <http://dx.doi.org/10.1098/rspb.2013.1684>, 2013

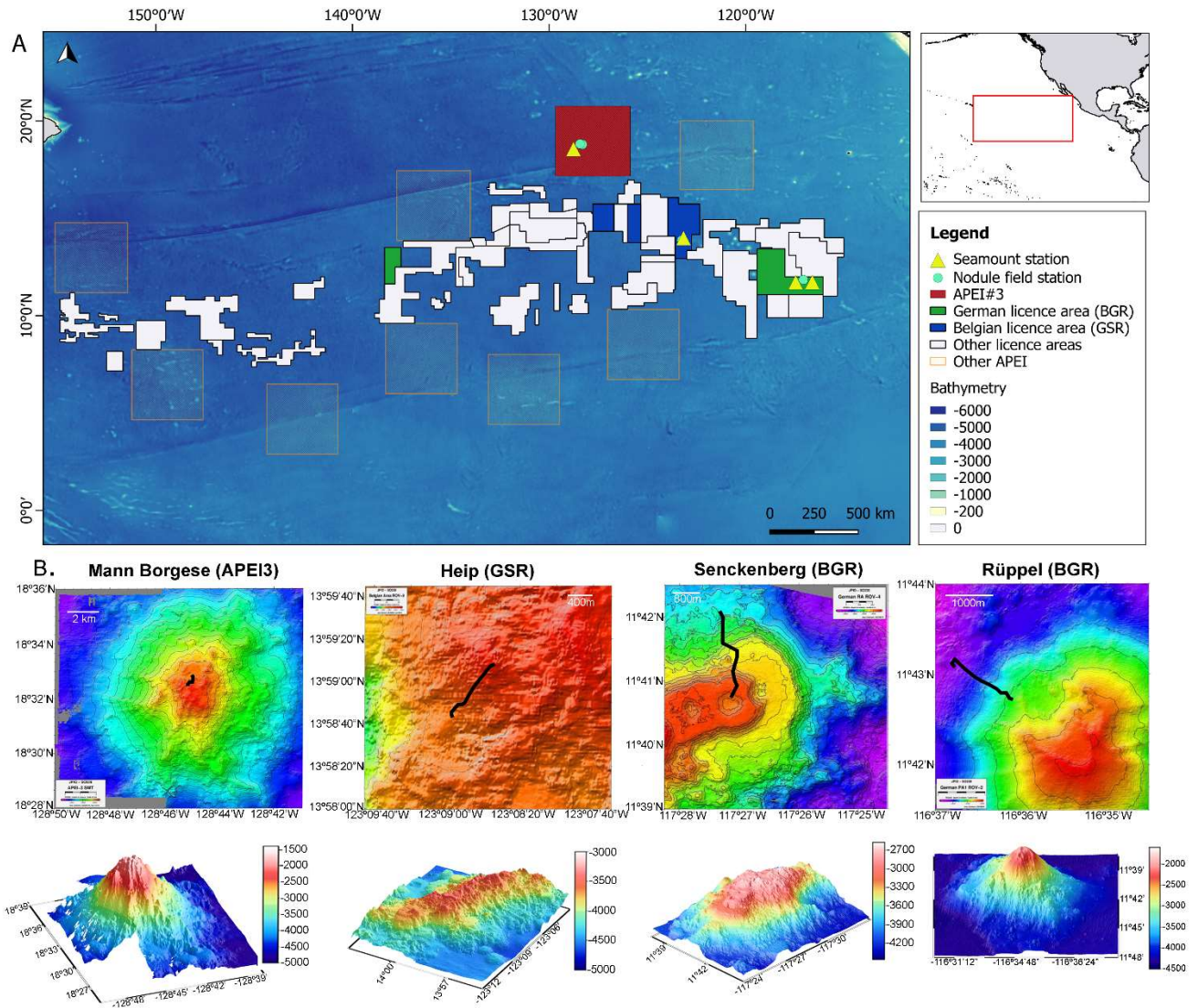
565 Wessel, P., Sandwell, D., and Kim, S.-S.: The Global Seamount Census. *Oceanography* 23(1), 24–33,  
566 <https://doi.org/10.5670/oceanog.2010.60>, 2010

## 568 Tables

569 Table 1: Overview table on details of imagery transects analysed in the Clarion-Clipperton license  
570 areas. Video duration includes time spent sampling. Number of observations include undetermined  
571 organisms. Transect lengths do not include parts visualising ancient disturbance tracks or parts when  
572 the seafloor was not visualised or visible.

Station/Dive	License Area	Seamount (SM) or Nodule field (NF)	Depth (m)	Video duration	Transect length	# obs/ dive	# obs /100m
SO239_29_ROV02	BGR	SM: Rüppell	3000-2500	7h47	1250m	429	34.3
SO239_41_ROV03	BGR	NF	4080-4110	6h32	1590m	932	58.6
SO239_54_ROV04	BGR	SM: Senckenberg	3350-2850	8h45	2500m	890	35.6
SO239_131_ROV08	GSR	NF	4470-4480	7h35	710m	445	62.8
SO239_135_ROV09	GSR	SM: Heip	3900-3550	7h35	1000m	359	35.9
SO239_141_ROV10	GSR	NF	4455-4480	7h35	520m	351	67.5
SO239_189_ROV13	APEI 3	NF	4890-4930	9h01	1790m	113	6.3
SO239_200_ROV14	APEI 3	NF	4650-4670	9h19	1490m	179	12.0
SO239_212_ROV15	APEI 3	SM: Mann Borgese	1850-1650	6h25	900m	378	42.0

573  
574  
575  
576  
577  
578  
579  
580  
581



583

584

585

586

587

588

589

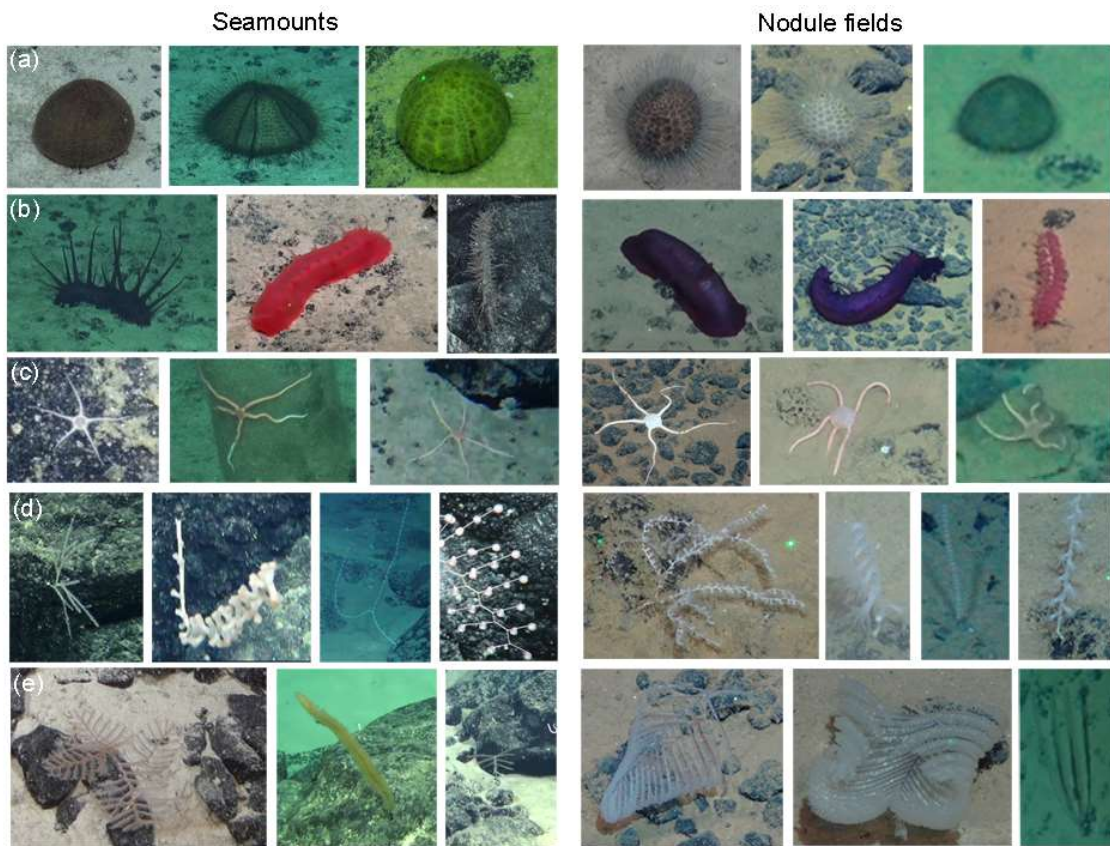
590

591

592

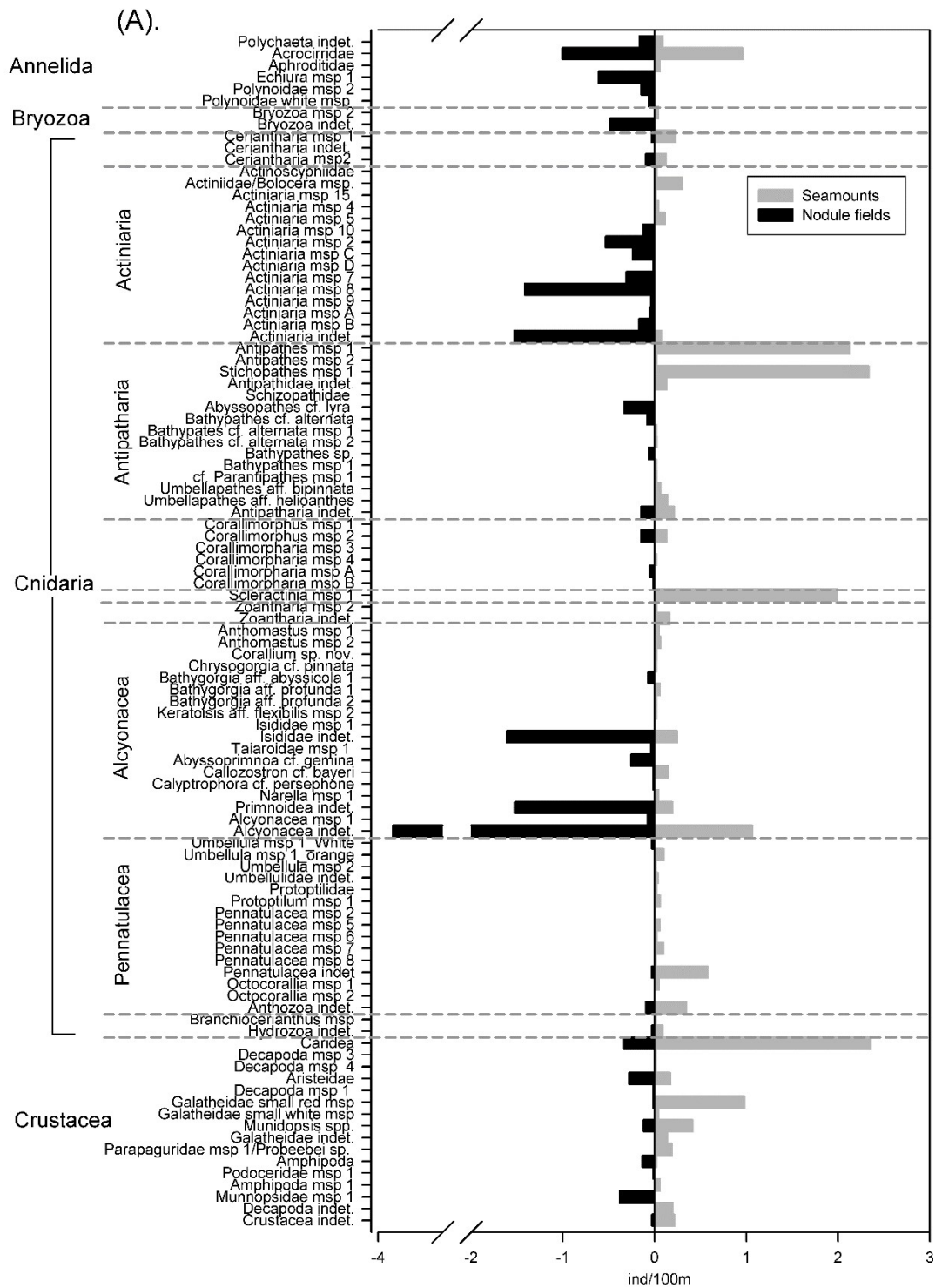
Fig. 1. (A). Location of the Clarion-Clipperton Fracture zone in the equatorial eastern Pacific Ocean featuring the contract areas from the International Seabed Authority (ISA) and the positions of the sampled areas (seamounts and nodule fields). Information on transect length and depth gradients can be found in Table 1. (B). Location of the seamount transects carried out towards the summit on the north –north-western flank and seamount profiles. Rüppel (BGR, ROV02) and Mann Borgese (APEI3, ROV15) are single seamounts, while Senckenberg (BGR, ROV04) and Heip (GSR, ROV09) are sea-mountain ranges.

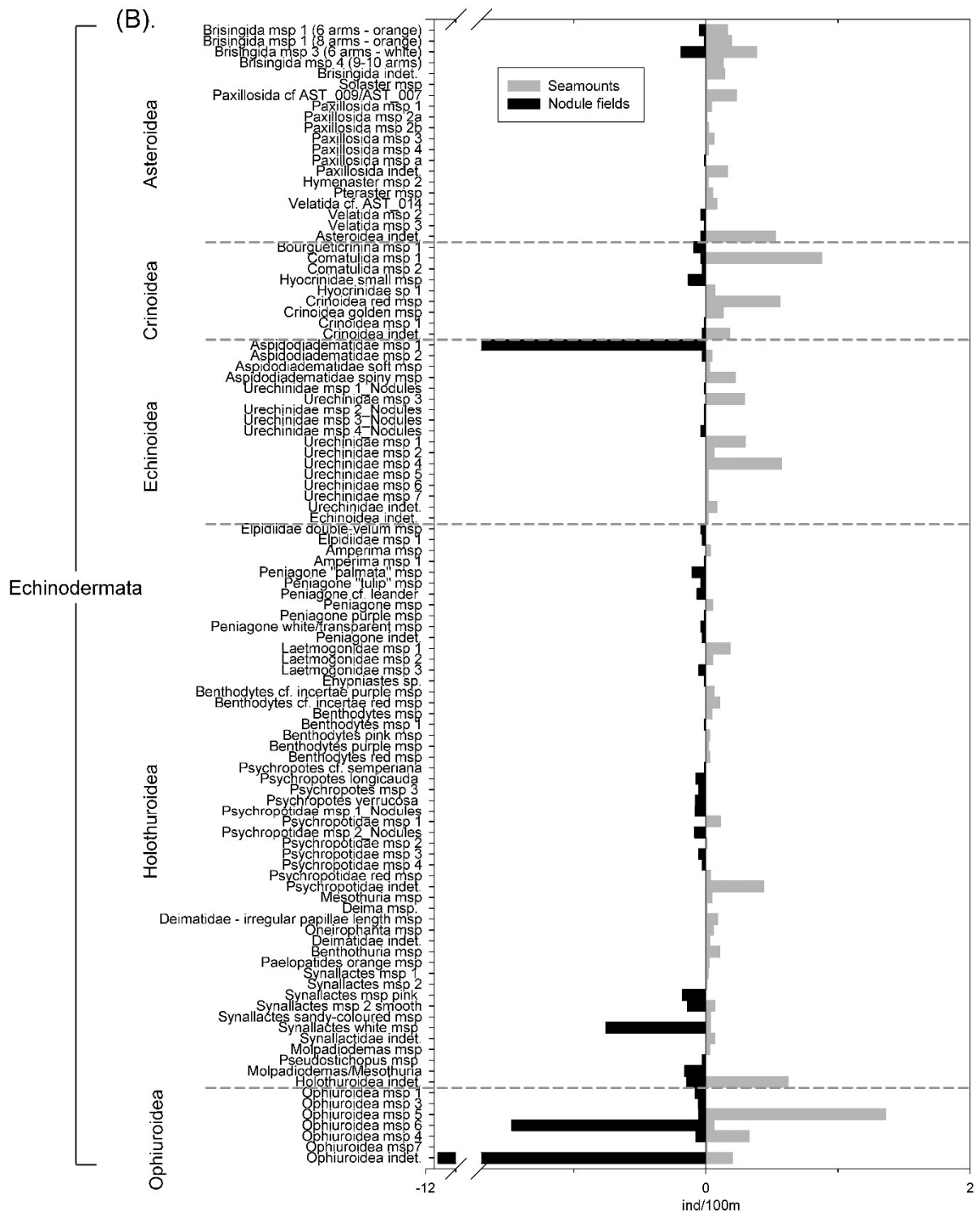


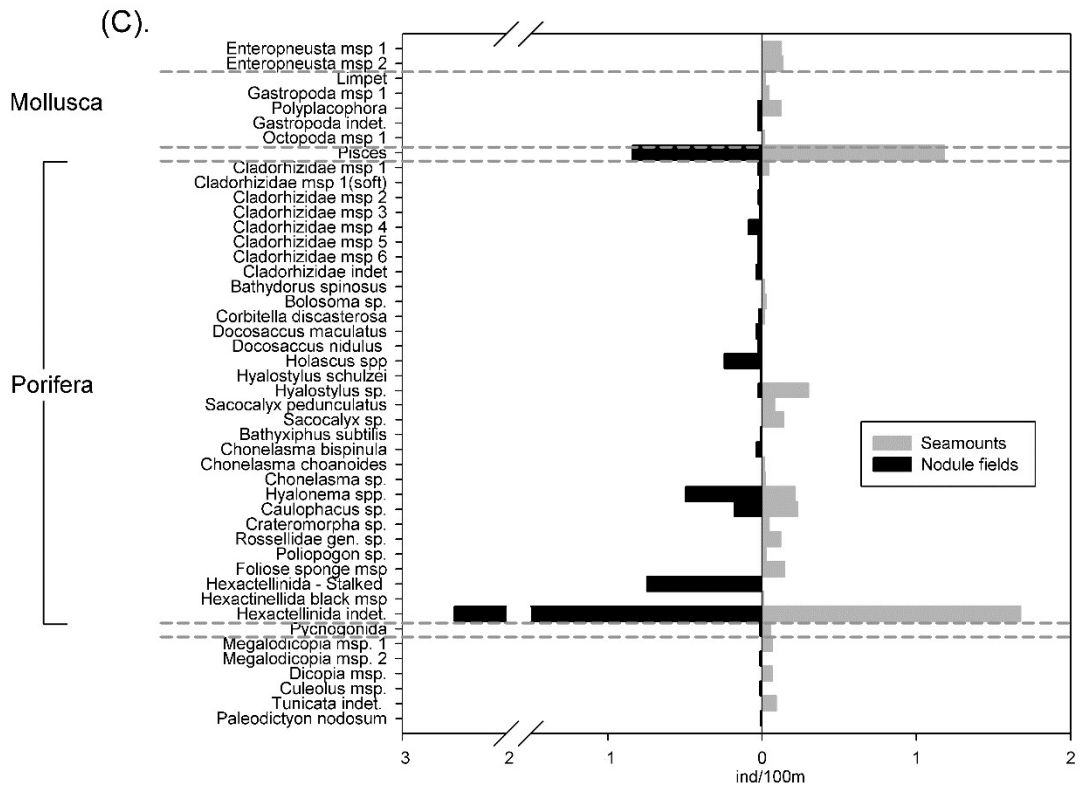


593  
 594 Fig. 2. Some examples of different morphospecies at seamounts and nodule fields in the CCZ.  
 595 Selected taxa were (a) Echinoidea (from left to right, Urechinidae msp 4 (URC\_019), Urechinidae msp  
 596 2 (URC\_013), Urechinidae msp 3 (URC\_009), Urechinidae msp. A (URC\_020), Urechinidae msp. B  
 597 (URC\_021), Urechinidae msp. C (URC\_005), (b) Holothuroidea (from left to right, Psychropotidae  
 598 msp 1 (HOL\_088), *Benthodytes* red msp. (HOL\_101), Deimatidae - irregular papillae msp. (HOL\_070),  
 599 *Psychropotes verrucosa* (HOL\_045), Laetmogonidae (HOL\_030), *Synallactes* msp 2 pink (HOL\_008)(c)  
 600 Ophiuroidea (from left to right, Ophiuroidea msp. 5 (OPH\_003), Ophiuroidea msp. 4 (OPH\_005),  
 601 Ophiuroidea msp. 6 (OPH\_006), Ophiuroidea msp. 6 (OPH\_006), Ophiuroidea (OPH\_012),  
 602 Ophiuroidea msp. 4 (OPH\_005)), (d) Alcyonacea (from left to right, *Callozostzon* cf. *bayeri* (ALC\_009),  
 603 *Bathygorgia* aff. *profunda* 2 (ALC\_005), *Keratoisis* aff. *flexibilis* msp 2 (ALC\_029), *Chrysogorgia* cf.  
 604 *pinnata*, *Abyssoprinnia* cf. *gemina* (ALC\_008), *Bathygorgia* aff. *profunda* 1, *Calyptrophora* cf.  
 605 *persephone* (ALC\_007), *Bathygorgia* aff. *abyssicola* 1 (ALC\_003), (e) Antipatharia (*Umbellapathes* aff.  
 606 *helioanthes* (ANT\_018), cf. *Parantipathes* morphotype 1 (ANT\_017), *Bathypates* cf. *alternata* msp 1  
 607 (ANT\_010), *Bathypathes* cf. *alternata* (ANT\_006), *Abyssopathes* cf. *lyra* (ANT\_022), *Bathypathes* sp.  
 608 (ANT\_003)). Codes refer to an ongoing collaboration in creating one species catalogue for the CCZ  
 609 and align all morphospecies of different research groups. Copyright: SO239, ROV Kiel 6000, GEOMAR  
 610 Helmholtz Centre for Ocean Research Kiel







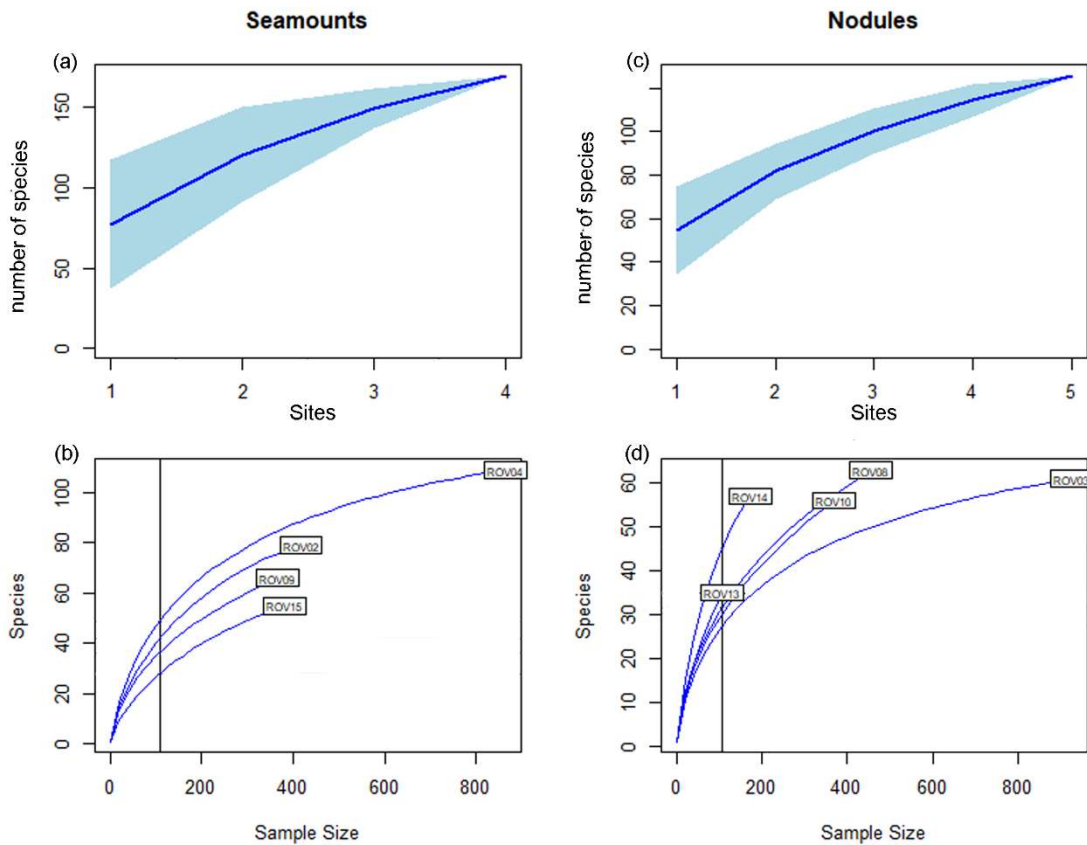


613

614 Fig. 3. Back-to-back histogram comparing average densities of morphospecies and taxa (ind/100m)  
 615 for seamount (#4) and nodule field (#5) video transects. (a) Annelida, Bryozoa, Cnidaria and  
 616 Crustacea, (B) Echinodermata and (C) Mollusca, Porifera, Hemichordata and Chordata (Tunicata).

617

618

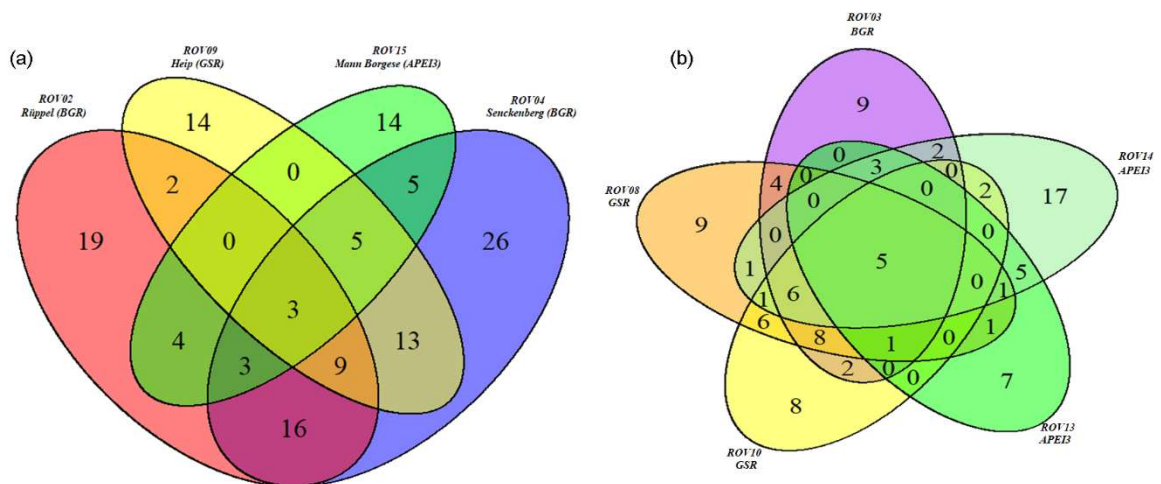


619  
 620 Fig. 4. Species accumulation (upper panel, a and c) and rarefaction curves (lower panel, b and d) for  
 621 the seamount (#4) and nodule field (#5) transects. Seamount dives: ROV02= Rüppel (BGR),  
 622 ROV04=Senckenberg (BGR), ROV09=Heip (GSR), ROV15=Mann Borgese (APEI3) in the lower left  
 623 panel (b). Nodule field dives: ROV03 was carried out in the BGR area, ROV08 and 10 in the GSR area  
 624 and ROV13 and 14 in the APEI3, presented in the lower right panel (d). Sample size is the number of  
 625 individuals. Vertical line in the lower panel shows sample size=100.

626

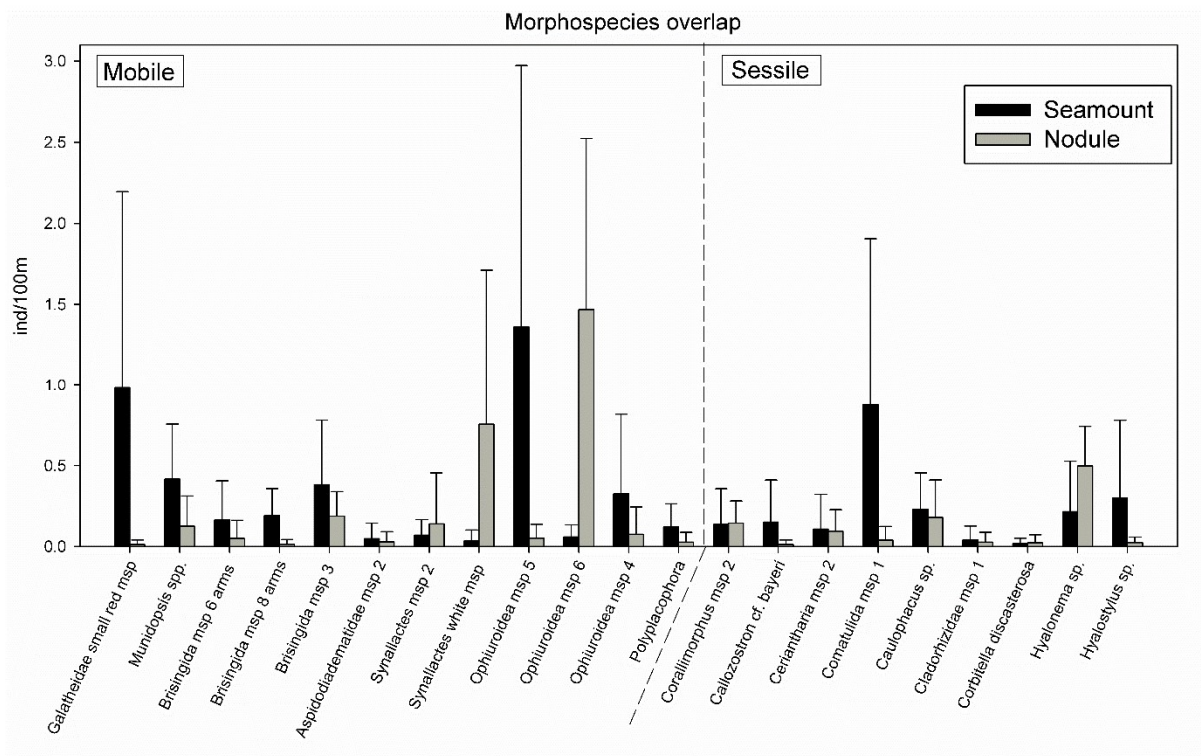
627

628



629  
 630 Fig. 5. A Venn diagram showing the unique and shared morphospecies among seamount video  
 631 transects. Values are indicative rather than absolute due to different transect lengths and  
 632 differences in richness. Left panel (a) features seamount transects and the right panel features the 5  
 633 nodule field transects. Colour codes were adapted among panels, with APEI3 nodule transects in  
 634 green, related to Mann Borgese seamount transect. BGR (ROV03) transect was purple in  
 635 correspondence to BGR seamount transects (red=Rüppel and blue=Senckenberg). GSR transects  
 636 (ROV08 and 09) were shades of yellow.

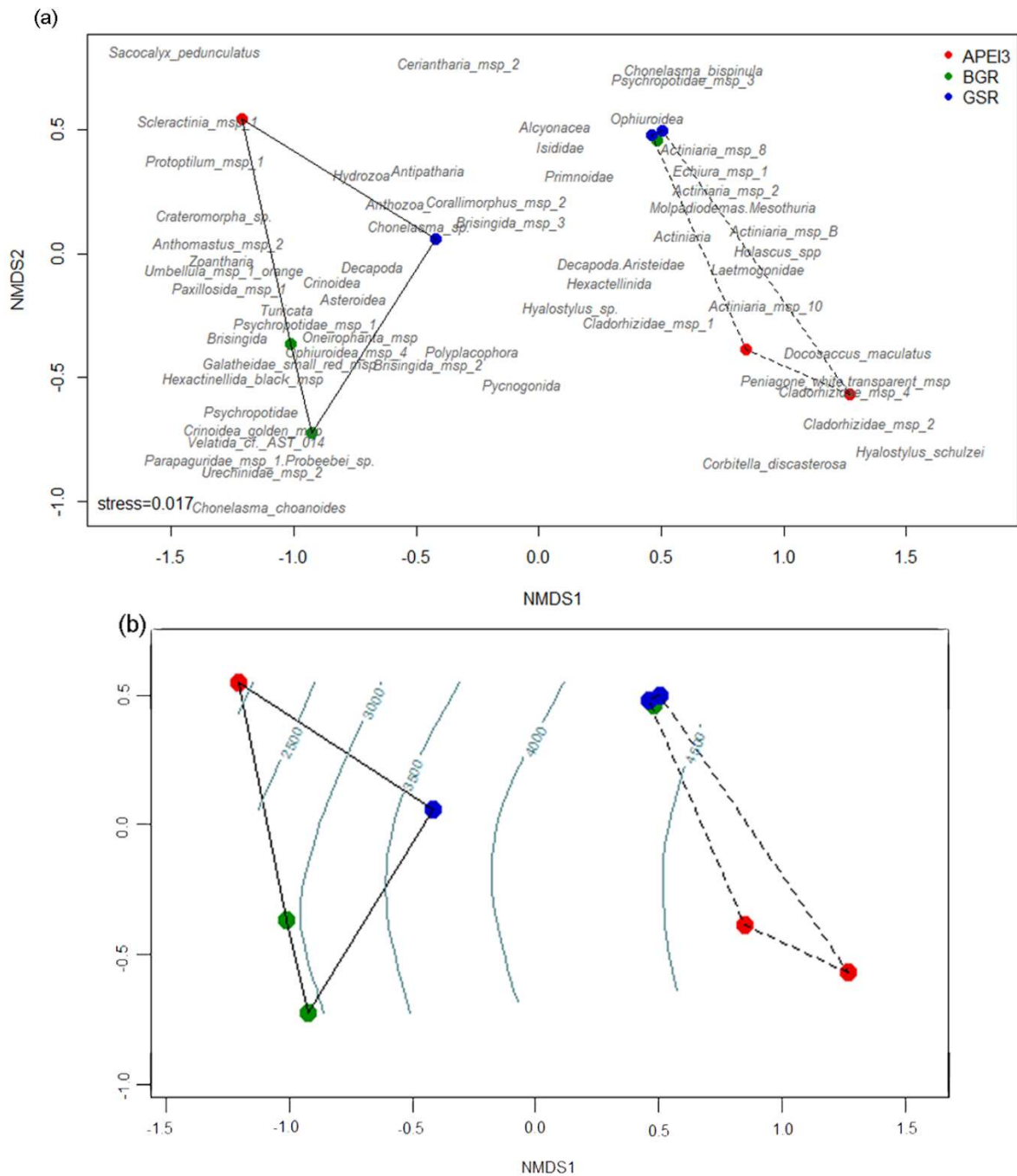
637  
 638  
 639  
 640  
 641



642

643 Fig. 6. Morphospecies present in both seamounts and nodule field transects and their average  
 644 density (ind/100m) and standard deviation per ecosystem.

645



646  
 647  
 648  
 649  
 650  
 651  
 652  
 653

Fig. 7. nMDS-plot with faunal densities and Bray-Curtis distances. Upper panel (a) presents the grouping of the video transects based on their faunal composition and lower panel (b) features the same plot but with depth as a vector fitting. Dotted lines group the nodule transects while the full line groups the seamount transects.

## Appendix

654

655 Table A1. Overview of all densities (ind./100m) observed within each video transect. Higher taxa are  
656 in bold. \* indicates taxa left out of the statistical analyses due to lack of representativity. Indets were  
657 organisms impossible to attribute to a lower taxonomic group. ROV02=Rüppel, ROV04=Senkcnberg,  
658 ROV09=Heip, ROV15=Mann Borgese



	SEAMOUNTS				NODULE FIELDS				
	ROV2 ind/100m	ROV4 ind/100m	ROV9 ind/100m	ROV15 ind/100m	ROV3 ind/100m	ROV8 ind/100m	ROV10 ind/100m	ROV13 ind/100m	ROV14 ind/100m
<b>Annelida*</b>									
<b>Polychaeta indet. *</b> (No Serpulidae)	0.14	0.12		0.11	0.31		0.38	0.06	0.07
Acrocirridae	0.14	0.16	3.56		0.57	0.14	0.58	1.79	1.95
Aphroditidae	0.20	0.04							
Echiura msp 1					0.57	1.13	1.15		0.20
Polynoidea									
Polynoidae msp 2						0.14	0.58		
Polynoidae white msp						0.14		0.06	0.13
<b>Bryozoa</b>									
Bryozoa msp 2			0.17						
Bryozoa indet.		0.038			0.44	1.55	0.19	0.11	0.13
<b>Cnidaria</b>									
<b>Anthozoa</b>									
<b>Ceriantharia</b>									
Ceriantharia msp 1	0.34	0.04	0.34	0.22					
Ceriantharia msp 2				0.43		0.28	0.19		
Ceriantharia indet.			0.08						
<b>Hexacorralia</b>									
<u>Actinaria</u>									
Actinoscyphiidae		0.12							
Actiniidae/ <i>Bolocera</i> msp.	1.02	0.19							
Actiniaria msp 15	0.07								
Actiniaria msp 4		0.08		0.11					
Actiniaria msp 5	0.07	0.08		0.32					

Actiniaria msp 10					0.31				0.34
Actiniaria msp 2					1.07	1.13	0.19		0.27
Actiniaria msp C					0.38	0.42	0.38		
Actiniaria msp D					0.06				
Actiniaria msp 7					0.63	0.14	0.58	0.06	0.13
Actiniaria msp 8					0.13	3.66	3.08		0.20
Actiniaria msp 9							0.19		
Actiniaria msp A							0.19		0.07
Actiniaria msp B					0.25	0.14	0.38	0.06	
Actiniaria indet.	0.14	0.15			1.57	1.41	4.42	0.11	0.13
<u>Antipatharia</u>									
Antipathidae									
<i>Antipathes</i> msp 1				8.49					
<i>Antipathes</i> msp 2				0.11					
<i>Stichopathes</i> msp 1				9.35					
Antipathidae indet.				0.54					
Schizopathidae									
<i>Abyssopathes</i> cf. <i>lyra</i>					0.50	0.56	0.58		
<i>Bathypathes</i> cf. <i>alternata</i>						0.14	0.19		0.07
<i>Bathypates</i> cf. <i>alternata</i> msp 1			0.08						
<i>Bathypathes</i> cf. <i>alternata</i> msp 2		0.12							
<i>Bathypathes</i> sp.					0.19	0.14			
<i>Bathypathes</i> msp 1			0.08						
cf. <i>Parantipathes</i> msp 1			0.11						
<i>Umbellapathes</i> aff. <i>bipinnata</i>		0.19	0.08						
<i>Umbellapathes</i> aff. <i>helioanthes</i>		0.58							
Antipatharia indet.	0.07	0.08	0.08	0.65	0.25	0.28	0.19		
<u>Corallimorpharia/Corallimorphidae</u>									
<i>Corallimorphus</i> msp 1		0.04	0.00						

<i>Corallimorphus</i> msp 2		0.46	0.08		0.25	0.28	0.19	
Corallimorpharia msp 3		0.04						
Corallimorpharia msp 4			0.08					
Corallimorpharia msp A					0.06		0.19	
Corallimorpharia msp B					0.06			
<u>Scleractinia</u>								
Scleractinia msp 1	0.14			7.85				
<u>Zoantharia</u>								
Zoantharia msp 2				0.11				
Zoantharia indet.		0.46		0.22				
<b>Octocorralia</b>								
<u>Alcyonacea</u>								
Alcyoniidae								
<i>Anthomastus</i> msp 1	0.20							
<i>Anthomastus</i> msp 2	0.00	0.15		0.11				
Coralliidae								
<i>Corallium</i> sp. nov.				0.11				
Chrysogorgiidae								
<i>Chrysogorgia</i> cf. <i>pinnata</i>			0.08					
Isididae								
<i>Bathygorgia</i> aff. <i>abyssicola</i> 1						0.14	0.19	
<i>Bathygorgia</i> aff. <i>profunda</i> 1		0.15	0.08					
<i>Bathygorgia</i> aff. <i>profunda</i> 2			0.08					
<i>Keratoisis</i> aff. <i>flexibilis</i> msp 2			0.08					
Isididae msp 1		0.04						
Isididae indet.	0.14		0.76	0.11	0.13	5.63	2.31	
Taiaroidea								
Taiaroidae msp 1							0.19	
Primnoidae								

<i>Abyssoprinoa</i> cf. <i>gemina</i>						0.70	0.58		
<i>Callozostxon</i> cf. <i>bayeri</i>	0.07	0.54			0.06				
<i>Calyptrophora</i> cf. <i>persephone</i>					0.06				
<i>Narella</i> msp 1		0.08		0.11					
Primnoidea indet.	0.61		0.17		2.70	3.38	1.54		
Alcyonacea msp 1					0.13			0.11	0.13
Alcyonacea indet.		0.15	1.44	2.69	8.93	6.62	4.04		0.07
<u>Pennatulacea</u>									
Umbellulidae									
<i>Umbellula</i> msp 1_White									0.13
<i>Umbellula</i> msp 1_orange		0.31		0.11					
<i>Umbellula</i> msp 2		0.08							
Umbellulidae indet.		0.15							
Protoptilidae				0.11					
Protoptilum msp 1		0.04		0.22					
Pennatulacea msp 2		0.04							
Pennatulacea msp 5		0.23							
Pennatulacea msp 6		0.12							
Pennatulacea msp 7		0.38							
Pennatulacea msp 8		0.08							
Pennatulacea indet	0.14	2.08		0.11		0.14			
Octocorallia msp 1				0.22					
Octocorallia msp 2									
Anthozoa indet.	0.14	0.12	0.51	0.65	0.13	0.14	0.19		
<b>Hydrozoa</b>									
<i>Branchiocerianthus</i> msp		0.08							
Hydrozoa indet.		0.08	0.08	0.22		0.14			
<b>Crustacea*</b>									

<b>Decapoda</b>									
Caridea	3.47	2.54	3.22	0.22	0.19		1.15	0.11	0.20
Decapoda msp 3		0.08							
Decapoda msp 4	0.07								
Decapoda/Aristeidae	0.07	0.08		0.54	0.06	0.56	0.58	0.11	0.07
Decapoda msp 1								0.06	
Galatheidae									
Galatheidae small red msp	2.79	0.54	0.17	0.43	0.06				
Galatheidae small white msp	0.07	0.12							
Munidopsis spp.	0.82	0.35	0.51			0.42			0.20
Galatheidae indet.	0.14	0.15	0.17	0.11					
Parapaguridae									
Parapaguridae msp 1/ <i>Probeebei</i> sp.	0.54	0.23							
<b>Peracarida</b>									
Amphipoda			0.08		0.06	0.28		0.06	0.27
Podoceridae msp 1								0.06	
Amphipoda msp 1		0.08	0.17						
Isopoda									
Munnopsidae msp 1					0.57	0.42	0.19	0.17	0.54
Decapoda indet.		0.12	0.68						
Crustacea indet.	0.07	0.31	0.51						0.13
<b>Echinodermata</b>									
<b>Asteroidea</b>									
<u>Brisingida</u>									
Brisingida msp 1 (6 arms - orange)		0.15	0.51		0.25				
Brisingida msp 1 (8 arms - orange)	0.14	0.38	0.25						0.07
Brisingida msp 3 (6 arms - white)		0.38	0.93	0.22	0.19	0.42	0.19		0.13
Brisingida msp 4 (9-10 arms)	0.14	0.38							

Brisingida indet.	0.27	0.08		0.22				
<u>Paxillosida</u>								
<i>Solaster</i> msp		0.04						
Paxillosida cf AST_009/AST_007		0.50	0.42					
Paxillosida msp 1	0.07			0.11				
Paxillosida msp 2a		0.04						
Paxillosida msp 2b			0.08					
Paxillosida msp 3		0.08	0.17					
Paxillosida msp 4		0.08						
Paxillosida msp 1							0.06	
Paxillosida indet.		0.65						
<u>Velatida</u>								
Pterasteridae								
<i>Hymenaster</i> msp 2	0.07							
<i>Pteraster</i> msp	0.20							
Velatida cf. AST_014	0.14	0.19						
Velatida msp 2						0.19		
Velatida msp 3								0.07
Asteroidea indet.	0.48	0.42	1.10	0.11	0.19			
<b>Crinoidea</b>								
<u>Comatulida</u>								
Bourgueticrinina msp 1					0.31			0.13
Comatulida msp 1	1.97	1.54				0.19		
Comatulida msp 2								0.13
<u>Hyocrinida</u>								
Hyocrinidae small msp					0.38	0.28		
Hyocrinidae msp 1		0.19	0.08	0.00				
Crinoidea red msp	0.20	1.62		0.43				
Crinoidea golden msp	0.14	0.38						

Crinoidea msp 1									0.07
Crinoidea indet.	0.07	0.46	0.08	0.11		0.14			
<b>Echinoidea</b>									
Aspidodiadematidae									
Aspidodiadematidae msp 1					3.96	2.68	2.31		
Aspidodiadematidae msp 2		0.19				0.14			
Aspidodiadematidae soft msp				0.11					
Aspidodiadematidae spiny msp	0.14			0.75					
Urechinidae									
Urechinidae msp 1_Nodules									0.07
Urechinidae msp 3	0.20	0.04	0.93						
Urechinidae msp 2_Nodules									0.07
Urechinidae msp 3_Nodules					0.06				
Urechinidae msp 4_Nodules							0.06		0.13
Urechinidae msp 1	0.20	0.73	0.25						
Urechinidae msp 2	0.20	0.04							
Urechinidae msp 4	0.48	1.38	0.42						
Urechinidae msp 5	0.07								
Urechinidae msp 6	0.07								
Urechinidae msp 7	0.07								
Urechinidae indet.	0.14	0.12	0.08						
Echinoidea indet.	0.07								
<b>Holothuroidea</b>									
<u>Elasipodida</u>									
Elpidiidae									
Elpidiidae double-velum msp							0.19		
Elpidiidae msp 1								0.06	0.07
<i>Amperima</i> msp	0.14								
<i>Amperima</i> msp 1					0.06				

<i>Peniagone</i> "palmata" msp						0.14	0.38		
<i>Peniagone</i> "tulip" msp							0.19		
<i>Peniagone</i> cf. <i>leander</i>						0.14	0.19		
<i>Peniagone</i> msp	0.14	0.08							
<i>Peniagone</i> purple msp									0.07
<i>Peniagone</i> white/transparent msp					0.06			0.06	0.07
<i>Peniagone</i> indet.					0.13				
Laetmogonidae									
Laetmogonidae msp 1	0.27	0.46							
Laetmogonidae msp 2	0.20								
Laetmogonidae msp 3							0.19		0.07
Pelagothuriidae									
<i>Eynpniastes</i> sp.									0.07
Psychropotidae									
<i>Benthodytes</i> cf. <i>incertae</i> purple msp		0.15	0.08						
<i>Benthodytes</i> cf. <i>incertae</i> red msp		0.42							
<i>Benthodytes</i> msp		0.19							
<i>Benthodytes</i> msp 1									0.07
<i>Benthodytes</i> pink msp				0.11					
<i>Benthodytes</i> purple msp			0.08						
<i>Benthodytes</i> red msp		0.04	0.08						
<i>Psychropotes</i> cf. <i>semperiana</i>								0.06	
<i>Psychropotes</i> <i>longicauda</i>							0.38		
<i>Psychropotes</i> msp 3					0.06		0.19		
<i>Psychropotes</i> <i>verrucosa</i>					0.25	0.14			
Psychropotidae msp 1_Nodules					0.06	0.14	0.19		
Psychropotidae msp 1		0.35	0.08						
Psychropotidae msp 2_Nodules						0.42			
Psychropotidae msp 2		0.04							



Psychropotidae msp 3					0.13	0.14		
Psychropotidae msp 4						0.14		
Psychropotidae red msp	0.14							
Psychropotidae indet.	1.22	0.42		0.11				
<u>Holothuriida</u>								
Mesothuriidae								
<i>Mesothuria</i> msp	0.07	0.12						
<u>Synallactida</u>								
Deimatidae								
<i>Deima</i> msp.		0.04						
Deimatidae - irregular papillae length msp		0.27	0.08					
<i>Oneirophanta</i> msp	0.07		0.17					
Deimatidae indet.		0.04	0.08					
Synallactidae								
<i>Benthothuria</i> msp				0.43				
<i>Paelopatides</i> "orange" msp	0.07	0.04						
<i>Synallactes</i> msp 1 (Synallactidae purple msp)	0.07							
<i>Synallactes</i> msp 2		0.04						
<i>Synallactes</i> msp 2 pink					0.13	0.56	0.19	
<i>Synallactes</i> msp 2 pink (smooth)	0.20	0.08				0.70		
<i>Synallactes</i> sandy-coloured msp	0.14							
<i>Synallactes</i> white msp	0.14				2.33	0.42	0.96	0.07
Synallactidae indet.	0.27							
<u>Persiculida</u>								
Molpadiodemidae								
Molpadiodemasp		0.12						
Pseudostichopodidae								
Pseudostichopus msp						0.14		
Molpadiodemasp/Mesothuria					0.19	0.28	0.19	0.13

Holothuroidea indet.	1.29	0.73	0.25	0.22	0.19	0.14	0.38		
<b>Ophiuroidea</b>									
Ophiuroidea msp 1					0.06	0.14	0.19		
Ophiuroidea msp 3						0.28			
Ophiuroidea msp 5	0.14	1.92	3.39					0.06	0.20
Ophiuroidea msp 6		0.15	0.08		1.07	2.96	2.12	0.34	0.87
Ophiuroidea msp 4	0.27	1.04			0.38				
Ophiuroidea msp7		0.04							
Ophiuroidea indet.		0.12	0.25	0.43	18.93	15.07	23.65		0.27
<b>Enteropneusta</b>									
Enteropneusta msp 1 cf. <i>Yoda</i>		0.50							
Enteropneusta msp 2 cf. <i>Saxipendum</i> msp.	0.54								
<b>Mollusca</b>									
<b>Gastropoda</b>									
Limpet			0.08						
Gastropoda msp 1			0.17						
Polyplacophora	0.27			0.22					0.13
Gastropoda indet.						0.14			
<b>Cephalopoda</b>									
Octopoda msp 1	0.07								
<b>Pisces*</b>	2.52	1.38	0.51	0.32	1.57	0.42	1.54	0.34	0.34
<b>Porifera</b>									
<b>Demospongiae</b>									
Cladorhizidae									
Cladorhizidae msp 1			0.17						0.13

Cladorhizidae msp 1(soft)									0.07
Cladorhizidae msp 2								0.06	0.07
Cladorhizidae msp 3									0.07
Cladorhizidae msp 4					0.06			0.11	0.27
Cladorhizidae msp 5						0.14			
Cladorhizidae msp 6						0.14			
Cladorhizidae indet								0.06	0.13
<b>Hexactellinida</b>									
Euplectellidae									
<i>Bathydorus spinosus</i>	0.07								
<i>Bolosoma</i> sp.				0.11					
<i>Corbitella discasterosa</i>	0.07							0.11	
<i>Docosaccus maculatus</i>						0.14		0.06	
<i>Docosaccus nidulus</i>						0.14			
<i>Holascusspp</i>					0.63	0.28	0.19	0.06	0.07
<i>Hyalostylus schulzei</i>								0.06	
<i>Hyalostylus</i> sp.		0.08	1.02	0.11				0.06	0.07
<i>Sacocalyx pedunculatus</i>				0.32					
<i>Sacocalyx</i> sp.	0.27	0.12	0.17						
Euretidae									
<i>Bathyxiphus subtilis</i>								0.06	
<i>Chonelasma bispinula</i>							0.19		
<i>Chonelasma choanoides</i>	0.07								
<i>Chonelasma</i> sp.			0.08						
Hyalonematidae									
<i>Hyalonema</i> spp.		0.08	0.68	0.11	0.38	0.70	0.77	0.17	0.47
Rosselidae									
<i>Caulophacus</i> sp.		0.31	0.51	0.11	0.57	0.14	0.19		
<i>Crateromorpha</i> sp.		0.08		0.11					

Rossellidae gen. sp.	0.27	0.04	0.17						
Pheronematidae									
<i>Poliopogon</i> sp.				0.11					
Hexactellinida/foliose sponge msp	0.07	0.12	0.08	0.32					
Hexactellinida - Stalked					0.88	1.13	1.73		
Hexactinellida black msp		0.04							
Hexactellinida indet.	1.50	1.00	3.56	0.65	3.27	2.39	5.19	0.89	0.74
<b>Pycnogonida</b>	0.14	0.00	0.08	0.00					0.07
<b>Tunicata</b>									
Octacnemidae									
<i>Megalodicopia</i> msp. 1	0.14	0.04	0.08						0.07
<i>Megalodicopia</i> msp. 2									
<i>Dicopia</i> msp.	0.27								
Pyuridae									
<i>Culeolus</i> msp.									0.07
Tunicata indet.	0.14	0.04	0.08	0.11					
<i>Paleodictyon nodosum</i>								0.06	

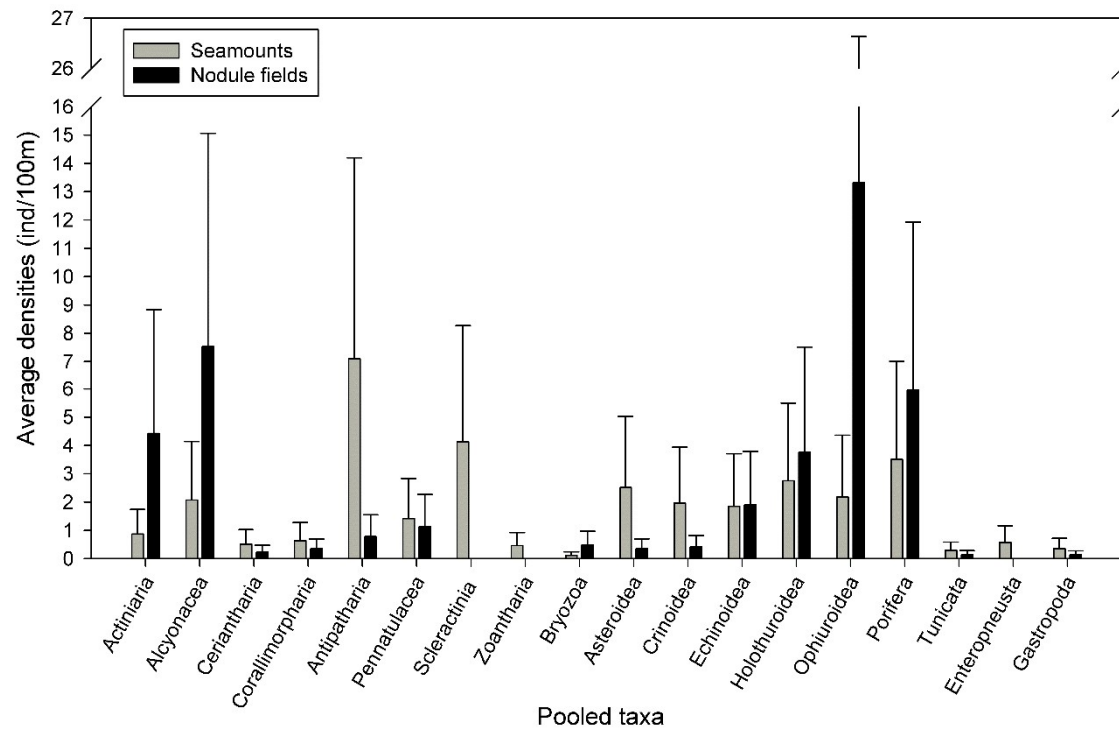


Fig. A1. Average densities at higher taxa level per ecosystem and standard deviation.